G-11

MICROSEISMS AND WATER WAVES

by

KERN KENYON

SUBMITTED IN PARTIAL FULFILLMENT OF THE
REQUIREMENTS FOR THE DEGREE OF
MASTER OF SCIENCE
and
BACHELOR OF SCIENCE

at the

MASSACHUSETTS INSTITUTE OF TECHNOLOGY

June, 1961

Signature of Author _____

Department of Geology and
Geophysics

Certified by _____

Thesis Supervisor

Accepted by _____

Chairman, Departmental Committee
on Graduate Students

ABSTRACT

MICROSEISMS AND WATER WAVES

by

Kern Kenyon

Submitted to the Department of Geology and Geophysics on May 22, 1961, in partial fulfillment of the requirements for the degree of Master of Science.

Part I investigates a possible instrument for detecting standing waves in deep water which is composed of three wave meters arranged in a triangle each of which measures the surface elevation as a function of time at one position. Four simple ideal ocean surfaces are investigated, and it is found that by examining the auto and crosscorrelations of the time series generated by the wave meters the instrument can detect the presence or absence of standing waves.

In Part II the following problem is investigated: If the ocean surface is composed of two infinite sine waves of the same frequency whose directions make an arbitrary angle β, does there exist a second order pressure variation which is independent of depth. The two simpler and well known limiting cases $\beta = 0$ (traveling wave) and $\beta = 180$ degrees (standing wave) are first reviewed. It is found that there will be no second order pressure variation at depth which might cause microseisms unless β is almost exactly 180 degrees.

In Part III microseism and water wave records from the Geophysical Field Station and weather data from the U. S. Naval Station, both in Bermuda, are investigated in a manner similar to that used by Kazi Haq. Amplitudes of water waves and microseisms are plotted for four storms which passed near Bermuda (one due to a hurricane and three due to cold fronts in which the isobars formed acute angles) and it was found that it is impossible that the microseisms could have been caused by wave action on shore. Some frequency spectra are computed from one storm and it is found that the frequency of the water waves is half that of the microseisms as predicted by theory in two out of three cases. The phenomenon of beats was discovered in both microseism and water wave records, and the period of the beats in the microseisms is half the period of the beats in the water waves.

Thesis Supervisor: Dr. Stephen M. Simpson
Assistant Professor of Geophysics

CONTENTS

ACKNOWLEDGEMENTS

The author wishes to express his sincere thanks to Dr. S. M. Simpson who supervised and sponsored this work, and without whose help, in fact, the third part of the thesis would not have been possible. The author feels grateful to two students, Jon Claerbout and Jim Galbraith who helped him with his computor program, and to Jackie Clark who did some of the tracing and tape to card converting for him. This work was done in part at the computation center at MIT, Cambridge, Massachusetts. The author also wishes to express his indebtedness to Mr. Frank Waltington who willingly shipped him 100 pounds of water wave, microseism, and weather data from Bermuda. This was made possible by Dr. Henry Stommel who kindly gave the permission to use his name.

INTRODUCTION

Most of this work was motivated by Kazi Haq's Ph.D. thesis on the nature and origin of microseisms.[2] He explains that the two main theories which try to explain the origin of microseisms are 1) that microseisms are caused by standing waves in the ocean and 2) that microseisms are caused by surf beating against the shore. He presents a convincing body of data in support of the first theory, but there are still a number of loose ends. One is that it is not possible to guarantee which microseism wave group corresponds to which water wave group. What Haq did was to assume that the ocean wave frequencies remain constant during a storm, and then carried out an approximate verification of the theory. Another loose end is that it is not clearly understood how or if the winds create standing waves during the special meteorological conditions under which microseisms are observed.

A more accurate verification of the theory could be made if there were an instrument which could guarantee that at a certain point in the ocean at a certain time standing waves existed. Several of these instruments could be scattered over the ocean surface, and as a storm or hurricane passed over each instrument would register the presence or absence of standing waves. Seismic stations at different points would record microseisms during this time, and the directions of travel of the microseisms

could be computed from the three components of ground motion measured by each seismograph. If it happened that the center of microseismic activity were located by two or three seismic stations at a region where one of these standing wave instruments happened to be, and if the instrument had registered the existence of standing waves at the appropiate time to have caused the microseisms, then the first theory would be almost verified. The finishing touch would be to check that the frequency of the micro-seism group was twice that of the standing wave group which produced the microseism group, as the theory of Longuet-Higgins predicts. PartI, then, discusses one possible standing wave instrument.

One special meteorological condition under which Kazi Haq and others (for a good reference list see Haq (2)) observed microseisms is a cold front moving rapidly over the ocean surface in deep water when the isobars which intersect the front form an acute angle. This means that the directions of the winds on either side of the front form an obtuse angle, and it is thought that in this case (2) that since large components of the winds are blowing in opposite directions, they might be effective in creating standing waves. It seems equally likely, however, that the winds might be effective in creating two wave trains whose directions would form the same obtuse angle that the wind directions form. Longuet-Higgins (6) shows that for a

single frequency if the obtuse angle is 180 degrees, i.e. a simple standing wave, then there exists a second order pressure variation which is independent of depth and which has a frequency of twice that of the standing wave; Longuet-Higgins[6] bases his theory of the origin of microseisms on this fact. It is also known (4, 6) that if the obtuse angle becomes zero degrees, i.e. simple traveling wave, then the pressure decays exponentially with depth, and it would be very unlikely that microseisms could be produced. It seemed interesting to investigate the intermediate case of an arbitrary obtuse angle to see if microseisms might possibly be produced in this case. Part II treats this case along with a review of the two special limiting cases.

In Part III the relationship between water waves and microseisms is studied by examining actual data. This problem has been worked on for the last fifty years, and consequently there exists a sizable body of literature on the subject. A good bibliography is contained in Kazi Haq's Ph.D. thesis (2). The present author has not made an extensive search of the work of others but has followed fairly closely the procedure used by Kazi Haq. This was felt to be worthwhile because the data used here comes from a different part of the world than that used by Haq. He used data taken off the East coast of the United States (Woods Hole, Mass.) where the water wave meter is quite some distance from the deep ocean, whereas the data used

here comes from Bermuda where the wave meter is quite close to deep water, and this does make some difference. The purpose in Part III is not to prove conclusively which of the two theories is correct, but to present some data which could be interpreted as evidence supporting the first theory.

PART I

Discussion of Standing Wave Instrument

The purpose of this part is to investigate a possible method for determining surface standing water waves at sea. The standing wave instrument proposed here will be composed of wave meters, each of which measures the surface elevation as a function of time at one point on the ocean surface. The author is not aware of any work similar to this which has been done. One might logically ask, why not put pressure gauges on the bottom? Since standing waves produce a second order pressure fluctuation which is independent of depth, standing waves should be detectable in principle by a pressure meter on the ocean floor. An answer might be that one would anticipate more practical difficulties with lowering an instrument to the bottom and getting it to pperate properly, and an instrument which works on the surface could be transported more readily from point to point.

Each wave meter in the instrument might be a float constrained to move along a vertical rod, for example. I will not discuss the design of such an instrument but rather give an idea of how many wave meters would be required and how far apart they should be spaced and then see what information the instrument will give for simple configurations of the ocean surface.

Keeping in mind a simplified picture of the ocean surface as a single frequency sine wave with a plane wave front, how many wave meters would be necessary to be able to determine if this sine wave is a traveling wave or a standing wave? Obviously one wave meter would not be enough unless it were placed at a node. For most cases two would be enough, because in general for a traveling wave the two meters would measure sine waves of the same amplitude with one out of phase with the other, whereas for a standing wave the two meters would measure different amplitudes and a phase difference of either zero degrees or 180 degrees. It could happen that the two meters lie along a line parallel to the wave fronts in which case the second meter gives no additional information. To be safe, then, there should be a minimum of three wave meters, and I suggest an equillateral triangle arrangement because there is really no point in using a general triangle. If two lie along a wave front, then the third will be sufficient in the most general case to be able to distinguish between the traveling and the standing wave.

The next question is how far apart should the three wave meters be spaced? If the direction of travel of the wave were at right angles to one side of the triangle and the projection of the other sides on the line of direction were a multiple of the wave length or if the direction of travel of the wave were parallel to one side of the triangle

and this side were an even multiple of the wave length, then a standing wave and a traveling wave would give identical recordings at all three wave meters. Careful consideration will show that if it can be guaranteed that a side of the triangle is less than one half the wave length of the sine wave, then the instrument will always be able to tell if the wave is a standing or a traveling wave. The most degenerate case is that in which two meters lie along a wave front and these two and the third are symmetric about a node or a line midway between two nodes. To the three meters a standing wave will look like a traveling wave as far as amplitude is concerned, but the phase difference between the first two meters and the third will tell the difference provided one side of the triangle is less than one half the wave length.

An upper and lower bound on the size of the triangle can be estimated. Including the effect of surface tension in deriving the equation of the free surface of a fluid from the linearized hydrodynamical equations will give a velocity of propogation for a sine wave[4] .

(1) $c^2 = (g/\alpha + T/\rho\alpha)\tanh\alpha h$

$\alpha = 2\pi/\lambda$ = wave number
$g = 980$ cm/sec^2
T = surface tension
ρ = density
h = depth of fluid

A plot of velocity against wave length will have a minimum, and for wave lengths greater than this minimum the waves are governed primarily by gravity; for wave lengths less than the minimum the waves or ripples are primarily governed by the surface tension. In deep water where $\tanh \alpha h \approx 1$ (this is to be taken as the definition of deep water) and $T/\rho \approx 70$ cm / sec^2 for water, Cmin 23cm/sec, and $\lambda_{min} \approx 1.5$cm. This would be the lower limit for the triangle side since the interest is in gravity waves. A rough upper bound can be found from the fact that the average frequency of storm waves measured from power spectra computed by Kazi Haq is roughly 0.12 cycles/sec. For deep water gravity waves from (1) $c^2 = \frac{g\lambda}{2\pi} = (\lambda f)^2$ where f is frequency. This rough average frequency gives a rough average wave length of 8 meters; therefore if the triangle side were less than 4 meters, the instrument could detect standing waves during an average storm, still under the restriction that only one frequency is present. Within these limits it is conceivable that a manageable instrument could be made which could be easily transported by ship.

The standing wave instrument will now be assumed to consist of three wave meters at the three corners of an equilateral triangle, a side of which is less than half the wave length of the waves being measured. Each wave meter will record a time series, which for our purposes will be considered infinite in length. A technique for operating on these given time series to find out if standing waves are present will now be discussed.

Case 1) Single Frequency standing and traveling wave

The technique is that of auto and cross-correlations. Taking the surface of the ocean as the xy plane with z-axis positive upward, taking the simplest surface as a sine wave of single frequency w and amplitude A whose wave front is parallel to the y-axis, then the time series measured by the various wave meters will be:

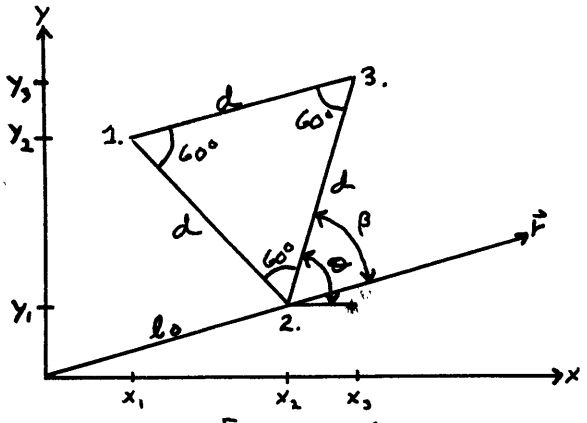

Figure 1.

	Standing Wave	Traveling Wave
Meter 1.	$f_1(t)=A_1\sin wt$	$A\sin(\alpha x_1-wt)$
" 2.	$f_2(t)=A_2\sin wt$	$A\sin(\alpha x_2-wt)$
" 3.	$f_3(t)=A_3\sin wt$	$A\sin(\alpha x_3-wt)$

where $A_i=A\sin\alpha x_i$ $i=1,2,3$. Write $A\sin(\alpha x_2-wt)$ as $A\sin(\alpha x_1+\delta_{21}-wt)$ etc., where $\delta_{21}=\alpha(x_2-x_1)$ etc., and we can take $x_1=0$ for traveling waves without loss of generality. The auto correlation function is defined as follows (5):

$$(2)\qquad \varphi_{ii}=\lim_{T\to\infty}\frac{1}{2T}\int_{-T}^{T} f_i(t)\,f_i(t+\tau)\,dt \qquad i=1,2,3$$

and the cross-correlation function is:

$$(3)\quad \varphi_{ij} = \lim_{T\to\infty} \frac{1}{2T}\int_{-T}^{T} f_i(t)\, f_j(t+\tau)\, dt \qquad i,j = 1,2,3 \qquad i \neq j$$

In this simple case the functions are periodic so that (2) may be written as:

$$(4)\quad \varphi_{ii} = \frac{1}{T}\int_{-T/2}^{T/2} f_i(t) f_i(t+\tau)\, dt \qquad T = 2\pi/\omega$$

with a similar change for the crosscorrelation. The auto and crosscorrelations are readily computed to be:

Standing Wave	Traveling Wave
$A_1^2/2\cos w$	$A_1^2/2\cos w\tau$
$A_2^2/2\cos w$	$A_2^2/2\cos w\tau$
$A_3^2/2\cos w$	$A_3^2/2\cos w\tau$
$A_1A_2/2\cos w$	$A_1^2/2\cos(w\tau+\delta_{21})$
$A_1A_3/2\cos w$	$A_1^2/2\cos(w\tau+\delta_{31})$
$A_2A_3/2\cos w$	$A_1^2/2\cos(w\tau+\delta_{31}-\delta_{21})$

In the degenerate case in which meters 1. and 2., say, lie along a line parallel to the wave fronts, then $\delta_{21}=0$ and $A_1 = A_2$.

Comparing the autocorrelations for the standing wave with those for the traveling wave show that both sets are cosine waves with angular frequency w but the three traveling wave autocorrelations have the same amplitude, whereas those for the standing wave all have different amplitudes in general. A comparison of the crosscorrelations shows that those for the traveling wave all have the same amplitude but each one has a different phase difference from the other two in general, whereas for the standing wave all three have diff-

erent amplitudes in general and phase differences of either zero or 180 degrees. (This may be seen by the fact that the product $A_1 A_2$ can be either positive or negative depending on whether αx_1 and αx_2 are both greater or less than 180 degrees or one is greater and the other less than 180 degrees etc.) Therefore, a computation of either the three auto or the three crosscorrelations will be sufficient to indicate whether the sine wave was a standing or a traveling wave, and this will be true for the degenerate case as well. Actual techniques for computing these functions for finite data will not be discussed; for a good summary see (3).

For the simple sine wave surface the velocity of propagation and the direction (not the sense) of the wave may be computed from knowing the time series from the three meters. For a traveling wave of frequency w the projection of the velocity along the sides 1,2 and 2,3 are (figure 1.)

(7) $V_{13} = c/\cos(\theta - 60^\circ) = \omega d/\delta_{31}$

(8) $V_{23} = c/\cos\theta = \omega d/\delta_{32}$

The phase differences δ_{21} etc. are found from the cross-correlations.

(9) $V_{13}/V_{23} = \cos\theta/\cos(\theta - 60^\circ) = \delta_{32}/\delta_{31}$

then

(10) $\tan\theta = \sqrt{3}/3\,[2\,\delta_{31}/\delta_{32} - 1]$

Solving for θ gives the direction of the wave, and together with w and d the velocity c can be found from either (7) or (8).

To determine the direction of a standing wave of frequency w and amplitude A, where r is the distance measured along the direction of travel $\vec{r}$ (figure 1.), the amplitudes measured by the three meters at any instant of time will be

(11) $z_1 = D \sin \alpha l_0$

(12) $z_3 = D \sin(\alpha l_0 + d \cos\beta)$ $\qquad D=2A\sin wt$

(13) $z_2 = D \sin(\alpha l_0 + d \cos(60^\circ + \beta))$

and for deep water waves there is a fourth equation

(14) $c^2 = g/\alpha \tanh \alpha h$

which becomes

(15) $\omega^2 = g\alpha$ $\qquad$ when $2\pi/\lambda >> 1$

Given w these four equations determine D, l_0, α, β from which the direction and the velocity of the wave may easily be found, and well as the amplitude A.

Also in this simple case the pressure fluctuations on the bottom may be colculated by a formula due to Longuet-Higgins (6)

(16) $$P(t) = d^2/dt^2 \; 1/\lambda \int_0^\lambda 1/2 z^2 dx$$

z is the form of the surface
P(t) is the pressure variation for infinite depth
$\lambda = 2\pi/\alpha$ is the wave length

If the auto and crosscorrelations indicate a traveling wave

is present, we know that there will be no pressure variation on the bottom, and this is readily verified by the above formula using $z=A\sin\alpha(x-ct)$. On the other hand if the auto and crosscorrelations tell us there is a standing wave present, we know there will be a secone order pressure variation on on the bottom. Using $z=2A\sin x \cos wt$ in (16) gives

$$P(t)=2A\ w\ \cos 2wt$$

which shows the two to one frequency relationship. This will be discussed further in Part II.

Case 2) Sum of Single Frequency Standing and Traveling Waves

Now imagine a slightly more complicated form for the ocean surface, that produced by the interference of two sine waves of the same frequency but different amplitudes traveling in opposite directions. This surface may be thought of equivalently as a superposition of a standing wave and a traveling wave. For simplicity take the direction of travel as the x-axis, the ocean surface still being the xy plane with z positive upward. Then

$$
\begin{aligned}
z &= A\sin\alpha(x-ct) + B\sin\alpha(x-ct) \\
&= A\sin\alpha(x-ct) + A\sin\alpha(x+ct) + (B-A)\sin\alpha(x+ct) \\
&= 2A\sin\alpha x\cos wt + D\sin\alpha(x+ct) \qquad D=B-A
\end{aligned} \tag{17}
$$

The three wave meters now measure the three time series as follows:

Meter 1. $f_1(t) = A_1\cos wt + D\sin\alpha(x_1+ct)$

" 2. $f_2(t) = A_2\cos wt + D\sin[\alpha(x_1+ct) + \delta_{21}]$

" 3. $f_3(t) = A_3\cos wt + D\sin[\alpha(x_1+ct) + \delta_{31}]$

where the notation $A_i = 2A\sin\alpha x_i$ and $\delta_{ji} = \alpha(x_j - x_i)$ is the same as before. The auto and crosscorrelations may now be worked out to be:

$$
\begin{aligned}
\varphi_{11} &= K_1\cos w\tau \\
\varphi_{22} &= K_2\cos w\tau \\
\varphi_{33} &= K_3\cos w\tau
\end{aligned} \tag{19}
$$

$$
\begin{aligned}
\varphi_{12} &= K_{21}\cos w\tau + K\cos(w\tau + \delta_{21}) \\
\varphi_{13} &= K_{31}\cos w\tau + K\cos(w\tau + \delta_{31}) \\
\varphi_{23} &= K_{32}\cos w\tau + K\cos(w\tau + \delta_{32})
\end{aligned} \tag{20}
$$

where $K_1 = 1/2\left[A_1^2 + A_1^2 D/A + D^2\right]$ etc., $K = AD$, and

$K_{21} = A\left[A\cos\delta_{21} - (D+A)\cos\alpha(x_2 + x_1)\right]$ etc.

The three autocorrelations (19) have different amplitudes in general (in the degenerate case two are the same) which would indicate the presence of a standing wave. The crosscorrelations show (20) a combination of the effects due to a standing wave and a traveling wave.

In this example it is more complicated to calculate the direction of travel of velocity of propagation from the auto and crosscorrelations. From (19) or (20) one immediately finds w, and if one plots equations (20) at $w\tau = 90$ degrees

$$(21) \qquad \begin{aligned} \varphi_{12} &= K\cos\delta_{21} \\ \varphi_{13} &= K\cos\delta_{31} \\ \varphi_{23} &= K\cos(\delta_{31}-\delta_{21}) \end{aligned} \qquad \text{at } w\tau = \pi/2$$

These equations may now be solved for the three unknowns K, δ_{21}, δ_{31}, and then the velocity and direction of the sine wave can be calculated as was done for the traveling wave in Case 1) by using the phase differences δ_{21}, δ_{31}. Knowing w and c then determines α, and having found the δ's and K, the effect of the second terms in (20) may be subtracted out. Then (20) become:

$$(22) \qquad \begin{aligned} \varphi_{12} &= K_{21} + K\cos\delta_{21} \\ \varphi_{13} &= K_{23} + K\cos\delta_{31} \\ \varphi_{23} &= K_{32} + K\cos\delta_{32} \end{aligned} \qquad \text{at } w\tau = 0$$

and these will determine A, D and therefore B, and x_1, say. Finally from (19) the values of A_1, A_2, A_3, may be found. In other words all the constants can be solved for, and in particular the wave velocity, wave length, and direction of travel can be determined.

The mean pressure on the bottom of the ocean may now be calculated from (16) to be:

$$P(t)=2AB\omega^2\cos\omega t$$

As far as the pressure on the bottom is concerned the opposing waves must be of the same frequency and must be traveling in exactly opposite directions (however see Part II) but need not have the same amplitude, which Longuet-Higgins pointed out (see (6)).

Case 3) Standing and Traveling Waves of Two or More Frequencies

The next more complicated case to be investigated is a surface composed of two standing or traveling waves of the same amplitude but different angular frequencies w_1 and w_2 both oriented along the x-axis.

$$(23) \qquad z=f(t)=2A(\sin\alpha_1 x\cos w_1 t + \sin\alpha_2 x\cos w_2 t)$$

Now the meters will record

$$(24) \qquad \begin{aligned} f_1(t) &= A_{11}\cos w_1 t + A_{21}\cos w_2 t \\ f_2(t) &= A_{12}\cos w_1 t + A_{22}\cos w_2 t \\ f_3(t) &= A_{13}\cos w_1 t + A_{23}\cos w_2 t \end{aligned}$$

where $A_{ij}=2A\sin\alpha_i x_j$; $i=1,2$; $j=1,2,3$. Now using equation (2) for the form of the autocorrelation, the three autocorrelations are computed to be:

$$(25) \qquad \begin{aligned} \varphi_{11} &= 1/2(A_{11}^2\cos w_1\tau + A_{21}^2\cos w_2\tau) \\ \varphi_{22} &= 1/2(A_{12}^2\cos w_1\tau + A_{22}^2\cos w_2\tau) \\ \varphi_{33} &= 1/2(A_{13}^2\cos w_1\tau + A_{23}^2\cos w_2\tau) \end{aligned}$$

since the cross terms vanish by the orthogonality of cosines. If the surface had been composed of two traveling waves of the same amplitude, i.e.

$$(26) \qquad z=f(t)=A\sin(\alpha_1 x - w_1 t) + \sin(\alpha_2 x - w_2 t)$$

then the autocorrelations would be:

$$(27) \qquad \varphi_{11} = A/2(\cos w_1\tau + \cos w_2\tau) = \varphi_{22} = \varphi_{33}$$

In other words for the traveling waves the autocorrelations are identical, but for the standing wave they are different. It is possible to extrapolate and say that if the ocean surface is composed of any number of pure traveling waves with the same direction, then the three autocorrelations of the three

time series produced by the three meters will be identical, whereas if the surface is composed of any number of pure standing waves with the same direction, the three autocorrelations will be different in general (at least two will differ in case of degeneracy). By pure traveling waves is meant any number of sine waves of different amplitudes and frequencies traveling in either the +x or -x directions, say, such that there are no waves of the same frequency traveling in opposite directions, and a pure standing wave is composed of two sine waves of the same frequency and amplitude traveling in opposite directions. The statement will also be true if the waves, standing or traveling, do not all have the same direction relative to each other, provided all the waves of the same frequency do travel in the same direction. The reason for this is that waves of the same frequency traveling in different directions may be combined in a special form as Case 4) points out, whereas waves of different frequencies act independently of one another.

The crosscorrelations for the two standing waves are of the form:

$$(28) \qquad \varphi_{ij} = 1/2\left[A_{ii}A_{ij}\cos w_i\tau + A_{ji}A_{jj}\cos w_j\tau\right] \qquad i \neq j$$

and those for the two traveling waves have the form:

$$(29) \qquad \varphi_{ij} = \hat{A}^2/2\left[\cos(w_i\tau + \delta_{ji}(w_i)) + \cos(w_j\tau + \delta_{ji}(w_j))\right]$$

$$\delta_{ji}(w_i) = \alpha_i(x_j - x_i) \quad \text{etc.}$$

The crosscorrelations contain information about the relative

phase difference for the two frequencies between the pairs of wave meters. The amplitude and phase spectrum may be obtained by taking the cosine and sine transform of the crosscorrelations as shown by Lee (5). For two standing waves (28) is an even function of the shift so its sine transform is zero. This fact indicates that the relative phase differences are either zero or 180 degrees which we know to be true for the standing wave. For the two traveling waves the phase differences are given by (see Lee (5))

$$\delta_{ij}(w_i) = \arctan\left\{\frac{\mathrm{Im}\left[\Phi_{12}(w_i)\right]}{\mathrm{Re}\left[\Phi_{12}(w_i)\right]}\right\} \tag{30}$$

and from these the wave directions for each frequency corresponding to a traveling wave may be calculated. When two or more standing waves are present it is too complicated, if not impossible, to find their orientations.

When there are two or more frequencies present in the ocean surface it is not possible to use equation (16) to find the pressure on the ocean floor, and the reason for this is the nonlinear nature of the equations involved (see Part II).

Case 4) Intermediate Case Between Single Frequency Standing and Traveling Wave

The last and probably the most interesting case to be examined is a surface composed of two sine waves of the same frequency and amplitude traveling in different directions, not necessarily opposite ones. Consider one wave traveling along the vector $\vec{r}_1$ and the other along $\vec{r}_2$ where the angle between $\vec{r}_1$ and $\vec{r}_2$ is β (see figure 2.). Picking a convenient coordinate system in which the y-axis bisects the angle β (the ocean surface is still the xy plane), the form of the surface is:

$$z = A\exp i\alpha(a_{11}x + a_{12}y - ct) + A\exp i\alpha(-a_{11}x + a_{12}y - ct)$$
$$= 2A\cos(\alpha a_{12}y - wt)\cos\alpha a_{11}x \qquad (31)$$

taking the real part, and where $a_{11} = \cos\theta$, $a_{12} = \sin\theta$. This surface has the form of a wave traveling in the positive y direction with velocity $c = w/\alpha a_{12} = w/\alpha\sin\theta$ whose amplitude varies in the x direction with a wave length $2\lambda a_{11} = 2\lambda\cos\theta$. In other words it looks like a traveling wave in the y direction and a standing wave in the x direction. $2\theta + \beta = \pi$ so when

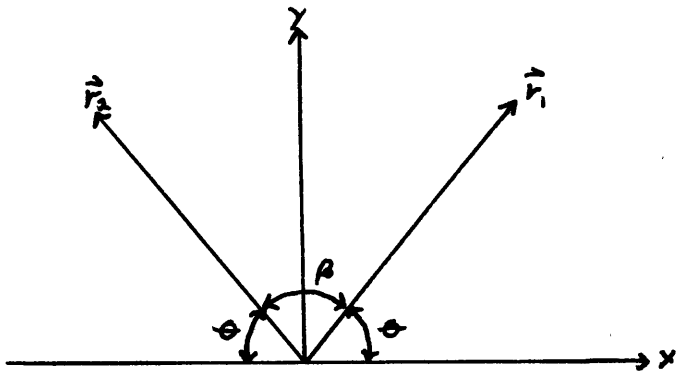

Figure 2.

$\beta = 0, \theta = \pi/2$, and the surface reduces to a simple traveling wave along the y-axis, and when $\beta = \pi$, $\theta = 0$, and the surface becomes a simple standing wave oriented along the x-axis. The three meters have coordinates (x_1, y_1), (x_2, y_2), (x_3, y_3), and they record the time series:

$$(32) \qquad z_i = 2A\cos(\alpha a_{12} y_i - wt)\cos\alpha a_{11} x_i \qquad i = 1,2,3$$

The autocorrelations are easily computed; they are:

$$(33) \qquad \varphi_{ii} = 2A^2\cos^2\alpha a_{11} x_i \cos w\tau \qquad i = 1,2,3$$

which are all different in general. This looks like the standing wave case; however, the crosscorrelations point out the difference.

$$(34) \qquad \varphi_{ij} = 2A^2\cos\alpha a_{11} x_i \cos\alpha a_{11} x_j \cos[\alpha a_{12}(y_j - y_i) - w\tau] \qquad i,j = 1,2,3 \quad i \neq j$$

Each crosscorrelation contains a phase $a_{12}\alpha(y_j - y_i)$ which in general is neither zero or 180 degrees, and for this reason this surface cannot be a simple standing wave. This surface cannot be a simple traveling wave either because (33) are in general all different. Thus on the basis of equations (33) and (34) it is possible to distinguish this surface from those of Case 1).

Other information about this surface may be found. The magnitude and direction (relative to the three wave meters) of the velocity c may be computed as in Case 1) from knowing the phase differences between the three pairs of meters, which are determined from the three equations (34). w is found from

either (33) or (34) and then from (15) α can be determined. Now $c=w/\alpha \sin\theta$ may be solved for θ which gives the directions of both sine waves relative to the wave meter network. This surface will be further discussed in Part II.

Conclusion

It is difficult to summarize the particular surfaces to which the standing wave instrument has been subjected; however, the general procedure for detecting standing waves is to first preform the operations of auto and cross-correlations on the three time series generated by the three wave meters under the assumption of infinite data. If all three autocorrelations are identical, one knows that there are no standing waves present. If all three autocorrelations differ among themselves and the crosscorrelations contain a phase which is either zero or 180 degrees, then one concludes that there is a standing wave present. These ideas were extrapolated to cover any number of all standing or all traveling waves. A mixture of standing and traveling waves was not discussed, but this case can be handled by taking the sine and cosine transforms of the crosscorrelations to sort out which frequencies correspont to traveling and which to standing waves. The intermediate case between a standing and a traveling wave shows up as just that when the auto and crosscorrelations are examined.

Other information such as the wave direction and velocity can be computed for any number of traveling waves but only for one standing wave, since the method is based on using the phase differences between the three meters. Also it is only in the case of a single standing wave that the mean pressure on the ocean bottom can be computed.

PART II

Setting up the Problem

The main subject of this part is a calculation of the second order pressure variation at the bottom of the ocean when the surface of the ocean has a form consisting of two infinite sine waves of the same frequency whose directions make an arbitrary angle β with each other. Two simpler well known cases will first be reviewed; they are 1) the case in which the surface is a single sine wave and 2) the case in which the surface is a simple standing wave. The interest in the first two cases is a check to see that the results of the third case reduce to those of the first two w when the angle β is zero and 180 degrees. The proceedure used here for the first two cases is undoubtedly in the literature, although I have not been able to find it. I have used a copy of notes taken by Professor Cantwell on a course on water waves given by Longuet-Higgins at MIT in 1958 as a guide.

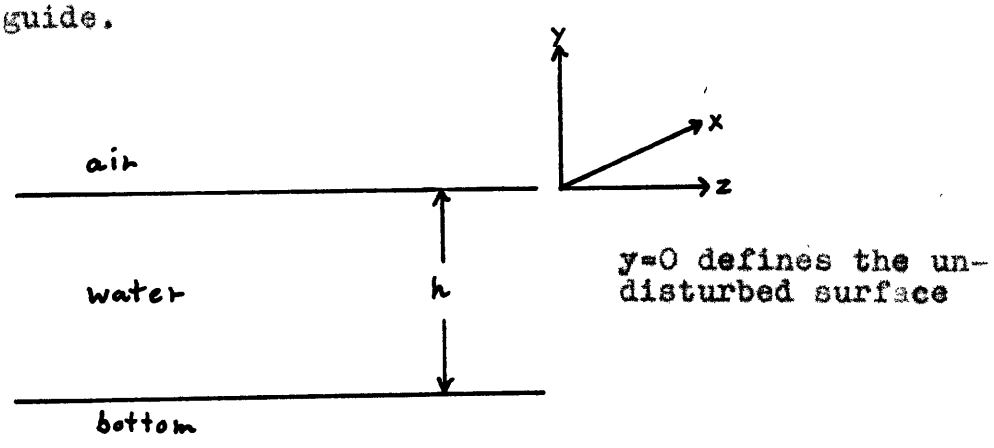

Figure 3.

The following may easily be found in Lamb (4). In order to set up the equations which govern the surface wave problem, the usual simplifying statements are first made that the fluid is incompressible and irrotational. the possible consequences of these assumptions will not be discussed. Under these conditions Euler's equations of motion for the fluid can be replaced by Bernoulli's equation, and the equation of continuity (conservation of mass) can be replaced by Laplace's equation for the velocity potential .

(1) $\nabla^2\varphi = 0$

This is the basic equation which governs the fluid.

The boundary conditions are three, one at the bottom, and two at the free surface. The boundary condition at the bottom is the statement that the component of the fluid velocity normal to the bottom must vanish at the bottom. It is expressed by

(2) $d\varphi/dy = \varphi_y = 0$ at $y=-h$

One of the free surface conditions is the one which states that a particle on the surface remains on the surface and is expressed by

(3) $DF/Dt = 0$ at $y=0$ $D/Dt = \partial/\partial t + (\vec{q}\cdot\vec{\nabla})$

F is the form of the surface; i.e. if the surface is given by $y=\eta(x,z,t)$, then $F=y-\eta(x,z,t)$. $\vec{q}=\vec{\nabla}\varphi$ is the velocity of the fluid. The other free surface boundary condition is the dynamic one which states that the pressure on either side of the surface must be equal to the same thing, namely zero. It

is expressed by Bernoulli's law in the form

(4) $g\eta + \varphi_t + 1/2(\varphi_x^2 + \varphi_y^2 + \varphi_z^2) = 0$ at $y=0$

φ is the velocity potential, g is gravity, η is the equation of the surface, and the subscripts refer to partial differentiation.

The following may be found in Stoker (page 20). The main difficulty is solving the water wave problem is that the two free surface boundary conditions are non linear. For example the kinematic condition (3) for a surface of the form $y=\eta(x,t)$ becomes:

(5) $\varphi_y = \eta_t + \eta_x \varphi_x$

In order to cope with the two non linear equations the following two perturbation series are assumed:

(6) $$\varphi = \varepsilon \varphi^{(1)} + \varepsilon^2 \varphi^{(2)} + \varepsilon^3 \varphi^{(3)} + \cdots$$
$$\eta = \varepsilon \eta^{(1)} + \varepsilon^2 \eta^{(2)} + \varepsilon^3 \eta^{(3)} + \cdots$$

where ε is a parameter which gives an idea of the scale or order of the term with which it is associated. When these expansions are inserted in (5) and like powers of ε are equated to zero, the result is:

(7) ε : $\varphi_y^{(1)} - \eta_t^{(1)} = 0$

(8) ε^2: $\varphi_y^{(2)} - \eta_t^{(2)} = \eta_x^{(1)} \varphi_x^{(1)} - \eta^{(1)} \varphi_{yy}^{(1)}$ at $y=0$

Third order terms will not be considered. Similarly (4) become:

(9) ε : $g\eta^{(1)} + \varphi_t^{(1)} = 0$

(10) ε^2: $g\eta^{(2)} + \varphi_t^{(2)} = -\eta^{(1)} \varphi_{ty}^{(1)} - 1/2\left[(\varphi_x^{(1)})^2 + (\varphi_y^{(1)})^2\right]$ at $y=0$

Equations (7) and (9) may be solved for $\varphi^{(1)}$ and $\eta^{(1)}$, then (8) and (10) may be solved for $\varphi^{(2)}$ and $\eta^{(2)}$, and in principle all the higher orders can be solved for by this procedure. Each $\varphi^{(k)}$ must then satisfy (1) and (2).

The ultimate interest here is in the second order pressure on the bottom. Pressure is calculated from Bernoulli's equation

(11) $\quad P/\rho + \varphi_t + 1/2(\varphi_x^2 + \varphi_y^2 + \varphi_z^2) + gy = \text{const.}$

P is the pressure and ρ is the fluid density. In general the constant may be a function of time only, and its only effect is to add a constant to the second order pressure. Since we are looking for second order pressure variations, a constant term is not of interest; therefore, it will be taken to be zero.

The procedure, then, is to assume a form for $\varphi^{(1)}$ and $\eta^{(1)}$ which satisfy (1) and (2), generate $\varphi^{(2)}$ from (8) and (10), and check that $\varphi^{(2)}$ also satisfies (1) and (2). Then $\varphi = \varepsilon\varphi^{(1)} + \varepsilon^2\varphi^{(2)}$. Put φ into (11) now to find the pressure; the pressure at the bottom is then found by setting y=-h.

Case 1) Single Frequency Traveling Wave

The first case to be considered is a surface whose form is a single frequency infinite progressive sine wave traveling in the positive x direction. This is a two dimensional surface $y = \eta(x,t)$. Assume to start with that

(12) $\varphi^{(1)} = A\cosh\alpha(y + h)\cos\alpha(x - ct)$

A is a constant amplitude
α is the wave number
h is the depth of the water
c is the velocity of propagation of the wave

$\varphi^{(1)}$ satisfies both (1) and (2) as is easy to check. Now $\eta^{(1)}$ is found from (7) to be

(13) $\eta^{(1)} = -(A/c)\sinh\alpha h\sin\alpha(x - ct)$

Longuet-Higgins assumes $\eta^{(1)}$ to be $\eta^{(1)} = a\sin\alpha(x - ct)$ and then finds $\varphi^{(1)}$ from (7) which is equivalent but physically more realistic. To relate the two procedures

(14) $A = -ac/\sinh\alpha h$

Now putting $\eta^{(1)}$ and $\varphi^{(1)}$ into (9) gives for the wave velocity:

(15) $c^2 = (g/\alpha)\tanh\alpha h$

Now from (8)

(16) $\varphi_y^{(2)} - \eta_t^{(2)} = \eta_x^{(1)}\varphi_x^{(1)} - \eta^{(1)}\varphi_{yy}^{(1)}$

(17) $\eta_x^{(1)}\varphi_x^{(1)} = (A^2\alpha^2/4c)\sinh 2\alpha h\sin 2\alpha(x - ct)$

(18) $\eta^{(1)}\varphi_{yy}^{(1)} = -(A^2\alpha^2/4c)\sinh 2\alpha h\sin 2\alpha(x - ct)$

Then putting (18) and (17) into (16), we get:

(19) $\varphi_y^{(2)} - \eta_t^{(2)} = (A^2\alpha^2/2c)\sinh 2\alpha h\sin 2\alpha(x - ct)$

Now working out the following:

(20) $(\varphi_x^{(1)})^2 = A^2\alpha^2\cosh^2\alpha h\,\sin^2\alpha(x - ct)$

(21) $(\varphi_y^{(1)})^2 = A^2\alpha^2\sinh^2\alpha h\,\cos^2\alpha(x - ct)$

(22) $h^{(1)}\varphi^{(1)}_{ty} = -A^2\alpha^2 \sinh^2\alpha h \sin^2\alpha(x-ct)$

Therefore, putting (20), (21), and (22) into (10), we get:

(23) $\varphi^{(2)}_t + g h^{(2)} = A^2\alpha^2 \{\sin^2\alpha(x-ct)[\sinh^2\alpha h - 1/2\cosh^2\alpha h] - 1/2\cos^2\alpha(x-ct)\sinh^2\alpha h\}$

Now differentiating (23) with respect to time gives:

(24) $\varphi^{(2)}_{tt} + g h^{(2)}_t = (A^2\alpha^2 w/2)\sin 2\alpha(x-ct)[\cosh^2\alpha h - 3\sinh^2\alpha h]$, $w = \alpha c$

Multiplying (19) by g and adding the result to (24) to eliminate $h^{(2)}_t$, and then substituting from (15) for g, we get:

(25) $\varphi^{(2)}_{tt} + g\varphi^{(2)}_y = (3A^2\alpha^2 w/2)\sin 2\alpha(x-ct)$

Now assume $\varphi^{(2)}$ is of the form

(26) $\varphi^{(2)} = K\cosh 2\alpha(y+h)\sin 2\alpha(x-ct)$

This satisfies (1) and (2) as required. Putting $\varphi^{(2)}$ into (25) and again using (15), we find:

$$K = -3A^2\alpha^2/8w\sinh^2\alpha h$$

$$\varphi^{(2)} = -(3A^2\alpha^2/8w\sinh^2\alpha h)\cosh 2\alpha(y+h)\sin 2\alpha(x-ct)$$

or using (14)

(27) $\varphi^{(2)} = -(3a^2 w/8\sinh^4\alpha h)\cosh 2\alpha(y+h)\sin 2\alpha(x-ct)$

This result agrees with Longuet-Higgins except for a term linear in t $-(a^2w^3/4\sinh^2\alpha h)t$ which is added to (37). This is a consequence of neglecting the constatn in equation (11). From (11) the first order pressure comes from $\varphi^{(1)}_t$ and is

(28) $P/\rho = -gy + (awc/\sinh\alpha h)\cosh\alpha(y+h)\sin\alpha(x-ct)$

For deep water, which is defined as $\lim h/\lambda \to \infty$, (28) becomes:

(29) $P/\rho = -gy + awc\exp\alpha y\sin\alpha(x-ct)$

This decreases exponentially with depth (negative y) and would be essentially zero at the bottom (y=-h). One term which contributes to the second order pressure is:

(30) $\varphi_t^{(2)} = (3a^2 w^2/4\sinh^4\alpha h)\cosh 2\alpha(y+h)\cos 2\alpha(x-ct)$

which becomes in deep water:

(31) $\varphi_t^{(2)} = (3a^2 w^2/4)[\exp 2\alpha(y-h)]\cosh 2\alpha(x-ct)$

and this certainly vanishes with depth. The linear term in t which does not appear in (27) would only contribute a constant term to the second order pressure since the time derivative is taken in (30). The two other terms which contribute to the second order pressure $(\varphi_x^{(1)})^2$ and $(\varphi_y^{(1)})^2$ also vanish with depth, which is just as easy to verify.

This is the well known result that at least as for as first and second orders are concerned the pressure on the bottom of the ocean is a constant function of time when an infinite sine wave travels in deep water. In other words it is extremely unlikely that microseisms could be caused by such a model of the ocean surface.

Case 2) Single Frequency Standing Wave

The second case to be investigated gives the well known amazing result that a standing wave at the surface does produce a second order pressure variation which is independent of depth and which has a frequency which is twice that of the standing wave. The procedure to be followed here is the same as in the first case but is slightly different from that used by Longuet-Higgins (6). $\varphi^{(1)}$ is now assumed to be:

(32) $$\varphi^{(1)} = A\cosh\alpha(y+h)\left[a_1\sin\alpha(x-ct) + a_2\sin\alpha(x+ct)\right]$$

i.e. a superposition of two sine waves of the same frequency and different amplitudes traveling in opposite directions along the x axis. Then from (7)

(33) $$h^{(1)} = (A/c)\sinh\alpha h\left[a_1\cos\alpha(x-ct) - a_2\cos\alpha(x+ct)\right]$$

Now working out the following expressions:

(34) $$h_x^{(1)}\varphi_x^{(1)} = (A^2\alpha^2/2c)\sinh 2\alpha h\left[a_1\cos\alpha(x-ct) + a_2\cos\alpha(x+ct)\right] \times\left[-a_1\sin\alpha(x-ct) + a_2\sin\alpha(x+ct)\right]$$

(35) $$h^{(1)}\varphi_{yy}^{(1)} = (A^2\alpha^2/2c)\sinh 2\alpha h\left[a_1\sin\alpha(x-ct) + a_2\sin\alpha(x+ct)\right] \times\left[a_1\cos\alpha(x-ct) - a_2\cos\alpha(x+ct)\right]$$

Combining (34) and (35) into (8) gives:

(36) $$\varphi_y^{(2)} - h_t^{(2)} = (A^2\alpha^2/2c)\sinh 2\alpha h\left[-a_1^2\sin 2\alpha(x-ct) + a_2^2\sin 2\alpha(x+ct)\right]$$

Now working out the following expressions:

(37) a) $$h^{(1)}\varphi_{ty}^{(1)} = A^2\alpha^2\sinh^2\alpha h\left[-a_1\cos\alpha(x-ct) + a_2\cos\alpha(x+ct)\right] \times\left[a_1\cos\alpha(x-ct) - a_2\cos\alpha(x+ct)\right]$$

b) $$(\varphi_x^{(1)})^2 = A^2\alpha^2\cosh^2\alpha h\left[a_1\cos\alpha(x-ct) + a_1\cos\alpha(x+ct)\right]^2$$

c) $$(\varphi_y^{(1)})^2 = A^2\alpha^2\sinh^2\alpha h\left[a_1\sin\alpha(x-ct) + a_2\sin\alpha(x+ct)\right]^2$$

Taking time derivatives of a), b), and c) and combining these with the time derivative of (10), we get:

(38) $$\varphi_{tt}^{(2)} + gh_t^{(2)} = (A^2\alpha^2 w/2)\left[a_1^2\sin 2\alpha(x-ct) - a_2^2\sin 2\alpha(x+ct) + 2a_1a_2\sin 2wt\right]\left[3\sinh^2\alpha h - \cosh^2\alpha h\right]$$

Multiplying (36) by g and adding the result to (38) to eliminate $h_t^{(2)}$ and then using (15) for g on the right side

(39) $$\varphi_{tt}^{(2)} + g\varphi_y^{(2)} = (A^2\alpha^2 w/2)[3a_1^2\sin 2\alpha(x-ct) - 3a_2^2\sin 2\alpha(x+ct) + 2a_1a_2(3\sinh^2\alpha h + \cosh^2\alpha h)\sin 2wt]$$

Now assume $\varphi^{(2)}$ has the form:

(40) $$\varphi^{(2)} = \cosh 2\alpha(y+h)[b_1\sin 2\alpha(x-ct) + b_2\sin 2\alpha(x+ct)] + b_3\sin 2wt$$

This sstisfies (1) and (2) as required. Putting $\varphi^{(2)}$ back into (40), using (15), and matching constants:

$$b_1 = -(3A^2\alpha^2a_1^2/8w\sinh^2\alpha h) \qquad b_2 = (3A^2\alpha^2a_2^2/8w\sinh^2\alpha h)$$

$$b_3 = (A^2\alpha^2a_1a_2/4w)(3\sinh^2\alpha h + \cosh^2\alpha h)$$

or using (14) and the identity:

(41) $$3\sinh^2\alpha h + \cosh^2\alpha h = \cosh 3\alpha h/\cosh\alpha h$$

$$b_1 = -(3a^2wa_1^2/8\sinh^4\alpha h) \qquad b_2 = (3a^2wa_2^2/8\sinh^4\alpha h)$$

$$b_3 = (a^2wa_1a_2\cosh 3\alpha h/4\sinh^2\alpha h\cosh\alpha h)$$

Therefore we have:

(42) $$\varphi^{(2)} = (a^2w/4\sinh^2\alpha h)\{[3\cosh 2\alpha(y+h)/2\sinh^2\alpha h][-a_1^2\sin 2\alpha(x-ct) + a_2^2\sin 2\alpha(x+ct)] + (a_1a_2\cosh 3\alpha h\sin 2wt/\cosh\alpha h)\}$$

This agrees with Longuet-Higgins again except for a term linear in t, which again is not bothersome for our purposes. In the deep water limit it is easy to see that $b_1 \to 0$, $b_2 \to 0$, and $b_3 \to a^2wa_1a_2$, so that (42) reduces to:

(43) $$\varphi^{(2)} = a^2wa_1a_2\sin 2wt$$

The second order pressure produced by this term is

(44) $$P/\rho = -\varphi_t^{(2)} - gy = -2a^2wa_1a_2\cos 2wt - gy$$

This is also the mean pressure along the bottom (i.e. in the x direction). The second order pressure produced by the terms

$(\varphi_x^{(1)})^2$ and $(\varphi_y^{(1)})^2$ as well as the first order pressure can be easily shown to vanish with depth (see (6)). Thus (44) shows the result that a standing wave at the surface produces a second order pressure variation which is independent of depth and has twice the frequency of the standing wave. Longuet-Higgins advanced his theory of the origin of microseisms (6) based on this idea. He also solved the compressible problem and showed that for certain depths there is a resonance effect which could boost the pressure at the bottom by a factor of five.

Case 3) Intermediate Case Between Single Frequency Standing and Traveling Wave

Imagine an idealized ocean surface to consist of two infinite sine waves of the same frequency and different amplitude whose directions make an arbitrary angle β with each other (see figure 2.). Since the angle β is always a positive angle between 0 and 180 degrees, the angle $\theta = (\pi-\beta)/2$ will always be positive. The ocean surface will now be the xz plane so z replaces y in figure 2.

The question to be asked is, could there exist a second order pressure variation which is independent of depth when the ocean surface has the form described above? The same procedure will now be followed as in the first two cases with slight modifications. Assume $\varphi^{(1)}$ has the form:

$$(45)\quad \varphi^{(1)} = B\cosh\alpha(y+h)\left[a_1\sin\alpha(x\cos\theta+z\sin\theta-ct) + a_2\sin\alpha(-x\cos\theta+z\sin\theta-ct)\right]$$

a_1 and a_2 are constants. This reduces to the previous expressions for $\varphi^{(1)}$ (12) and (32) when θ is put equal to 90 degrees (traveling wave in the z direction) and zero degrees (standing wave in the x direction). This form for $\varphi^{(1)}$ also satisfies (1) and (2) as it should. As before $h^{(1)}$ is found from (7)

$$(46)\quad h^{(1)} = (B/c)\sinh\alpha h\left[a_1\cos\alpha(x\cos\theta+z\sin\theta-ct) + a_2\cos\alpha(-x\cos\theta+z\sin\theta-ct)\right]$$

Equation (8) becomes modified because the surface is now a function of x,z,t (see Stoker page 20.)

$$(47)\quad \varphi_y^{(2)} - h_t^{(2)} = h_x^{(1)}\varphi_x^{(1)} + h_z^{(1)}\varphi_z^{(1)} - h^{(1)}\varphi_{yy}^{(1)} \quad \text{at } y=0$$

The expressions to be worked out are now more complicated.

$$(48)\quad h_x^{(1)}\varphi_x^{(1)} = (B^2\alpha^2/2c)\sinh 2\alpha h\cos^2\theta\{[a_1\cos\alpha(x\cos\theta+z\sin\theta-ct) - a_2\cos\alpha(-x\cos\theta+z\sin\theta-ct)][-a_1\sin\alpha(x\cos\theta+z\sin\theta-ct) + a_2\sin\alpha(-x\cos\theta+z\sin\theta-ct)]\}$$

$$(49)\quad h_z^{(1)}\varphi_z^{(1)} = (B^2\alpha^2/2c)\sinh 2\alpha h\sin^2\theta\{[a_1\cos\alpha(x\cos\theta+z\sin\theta-ct) + a_2\cos\alpha(-x\cos\theta+z\sin\theta-ct)][-a_1\sin\alpha(x\cos\theta+z\sin\theta-ct) - a_2\sin\alpha(-x\cos\theta+z\sin\theta-ct)]\}$$

$$(50)\quad h^{(1)}\varphi_{yy}^{(1)} = (B^2\alpha^2/2c)\sinh 2\alpha h\{[a_1\sin\alpha(x\cos\theta+z\sin\theta-ct) + a_2\sin\alpha(-x\cos\theta+z\sin\theta-ct)][a_1\cos\alpha(x\cos\theta+z\sin\theta-ct) + a_2\cos\alpha(-x\cos\theta+z\sin\theta-ct)]\}$$

Now combining (48), (49), and (50) into (47), we have:

$$(51)\quad \varphi_y^{(2)} - h_t^{(2)} = -(B^2\alpha^2/2c)\sinh 2\alpha h[a_1^2\sin 2\alpha(x\cos\theta+z\sin\theta-ct) + a_2^2\sin 2\alpha(-x\cos\theta+z\sin\theta-ct) + 2a_1a_2\sin^2\theta\sin 2\alpha(z\sin\theta-ct)]$$

Equation (10) becomes slightly modified to be:

$$(52)\quad \varphi_t^{(2)} + gh^{(2)} = -h^{(1)}\varphi_{ty}^{(1)} - 1/2\left[(\varphi_x^{(1)})^2 + (\varphi_y^{(1)})^2 + (\varphi_z^{(1)})^2\right] \quad \text{at } y=0$$

Working out the following expressions:

$$(53)\quad a)\ h^{(1)}\varphi_{ty}^{(1)} = -B^2\alpha^2\sinh^2\alpha h[a_1\cos\alpha(x\cos\theta+z\sin\theta-ct) + a_2\cos\alpha(-x\cos\theta+z\sin\theta-ct)]^2$$

$$b)\ (\varphi_x^{(1)})^2 = B^2\alpha^2\cos^2\theta\cosh^2\alpha h[a_1\cos\alpha(x\cos\theta+z\sin\theta-ct) + a_2\cos\alpha(-x\cos\theta+z\sin\theta-ct)]^2$$

$$c)\ (\varphi_z^{(1)})^2 = B^2\alpha^2\sin^2\theta\cosh^2\alpha h[a_1\cos\alpha(x\cos\theta+z\sin\theta-ct) + a_2\cos\alpha(-x\cos\theta+z\sin\theta-ct)]^2$$

$$d)\ (\varphi_y^{(1)})^2 = B^2\alpha^2\sinh^2\alpha h[a_1\sin\alpha(x\cos\theta+z\sin\theta-ct) + a_2\sin\alpha(-x\cos\theta+z\sin\theta-ct)]^2$$

Before combining (53) into (52) it is easier to take the time derivatives of both equations. Having done this, we get:

$$(54)\quad \varphi_{tt}^{(2)} + gh_t^{(2)} = (B^2\alpha^3c/2)\{[a_1^2\sin 2\alpha(x\cos\theta+z\sin\theta-ct) + a_2^2\sin 2\alpha(-x\cos\theta+z\sin\theta-ct)][3\sinh^2\alpha h - \cosh^2\alpha h] + [2a_1a_2\sin 2\alpha(z\sin\theta-ct)][3\sinh^2\alpha h + \cos 2\theta\cosh^2\alpha h]\}$$

Multiplying (51) by g and adding to (54) to eliminate and using (15), we get:

$$(55)\quad \varphi^{(2)}_{tt} + g\varphi^{(2)}_{y} = -(B^2\alpha^3 c/2)\{3a_1^2\sin 2\alpha(x\cos\theta + z\sin\theta - ct) + 3a_2^2\sin 2\alpha(-x\cos\theta + z\sin\theta - ct) - [2a_1a_2\sin 2\alpha(z\sin\theta - ct)]\times [3\sinh^2\alpha h + \cosh^2\alpha h(\cos^2\theta - 3\sin^2\theta)]\}$$

This also reduces to the equivalent statements (25) and (40) of the first two cases when θ is set equal to 90 degrees and zero respectively. $\varphi^{(2)}$ must now satisfy (1), (2), and (55). Assume $\varphi^{(2)}$ has the form:

$$(56)\quad \varphi^{(2)} = K_1\cosh 2\alpha(y+h)[a_1^2\sin 2\alpha(x\cos\theta + z\sin\theta - ct) + a_2^2\sin 2\alpha(-x\cos\theta + z\sin\theta - ct)] + K_2\cosh[2\alpha\sin\theta(y+h)][2a_1a_2\sin 2\alpha(z\sin\theta - ct)]$$

It is easy to check that this form for $\varphi^{(2)}$ will satisfy (1) and (2). Putting $\varphi^{(2)}$ into (55) and matching constants, we get:

$$K_1 = -(3B^2\alpha/8c\sinh^2\alpha h)$$

$$K_2 = (B^2\alpha/4c)\left[\frac{3\sinh^2\alpha h + \cosh^2\alpha h(\cos^2\theta - 3\sin^2\theta)}{(\sin\theta\sinh(2\alpha h\sin\theta)/\tanh\alpha h) - 2\cosh(2\alpha h\sin\theta)}\right]$$

or using (15) as before with $B = -ac/\sinh\alpha h$, these become:

$$K_1 = -(3a^2 w/8\sinh\alpha h)$$

$$K_2 = \left[\frac{a^2 w}{4\sinh\alpha h}\right]\left[\frac{3\sinh^2\alpha h + \cosh^2\alpha h(\cos^2\theta - 3\sin^2\theta)}{\sin\theta\cosh\alpha h\,\sinh(2\alpha h\sin\theta) - 2\sinh\alpha h\cosh(2\alpha h\sin\theta)}\right]$$

If θ is set equal to zero, $\varphi^{(2)}$ reduces to (42) by way of (41). Also if θ is set equal to 90 degrees and either a_1 or a_2 is chosen to be zero and the other to be a, then (56) reduces to the corresponding expression (28) in the traveling wave case with x replaced by z. For an arbitrary angle θ, $\varphi^{(2)}$ becomes:

$$(57)\quad \varphi^{(2)} = (-3a^2 w\cosh 2\alpha(y+h)/8\sinh^2\alpha h)[a_1^2\sin 2\alpha(x\cos\theta + z\sin\theta - ct) + a\sin 2\alpha(-x\cos\theta + z\sin\theta - ct)] + (a^2 w/4\sinh\alpha h)\times \left[\frac{3\sinh^2\alpha h + \cosh^2\alpha h(\cos^2\theta - 3\sin^2\theta)}{\sin\theta\cosh\alpha h\,\sinh(2\alpha h\sin\theta) - 2\sinh\alpha h\cosh(2\alpha h\sin\theta)}\right]\times [2a_1a_2\cosh(2\alpha\sin\theta(y+h))\sin 2\alpha(z\sin\theta - ct)]$$

In the deep water limit the first two terms of (57) become multiplied by $\exp[-2\alpha(y-h)]$ and therefore vanish with depth. Thus for deep water (57) becomes:

$$(58)\quad \varphi^{(2)} = 2a^2 w a_1 a_2 [\exp(2\alpha y \sin\theta)](\cos^2\theta/\sin\theta - 2)\sin 2\alpha(z\sin\theta - ct)$$

For $\theta = 0$ this reduces exactly to (43), which is the deep water limit for the standing wave case. One cannot set θ equal to 90 degrees, however, because (58) will be zero. If one puts θ equal to 90 degrees in (57) and then takes the deep water limit, the expression obtained will be identical to (31), which is the deep water limit for the traveling wave case. In the general case, noting that θ is always positive as explained earlier, we see that $\varphi^{(2)}$ decreases exponentially with increasing θ . For example, for waves of period 10 seconds and velocity 14 meters/second in water of depth 2,000 meters the exponential factor in (58) becomes:

1/e for θ = 0.11 degrees
0.1 for θ = 0.26 "
0.01 for θ = 0.80 "

The second order pressure variation calculated from (11) is proportional to $\varphi_t^{(2)}$, and except for extremely small values of θ , i.e. essentially standing waves, it will be vanishingly small. Therefore, it would seem very unlikely that microseisms would be produced by two sine waves of the same frequency, unless they traveled in almost exactly opposite directions, under the assumption of the idealized ocean surface considered.

It is easy to verify that the other second order pressure terms $(\varphi_x^{(1)})^2$ etc. and the first order pressure vanish with depth. The arguments of Longuet-Higgins (6) follow with slight modifications.

That (58) is a reasonable result can be seen by considering the potential energy of the surface. Longuet-Higgins relates the second time derivative of the potential energy of the surface to the pressure variation at the ocean bottom, and this is summarized by Haq (2). The potential energy P.E. is given by:

$$(59) \qquad P.E. = \tfrac{1}{2}\iint g\rho h^2 dz dx$$

ρ is the density of the fluid
h is the height of the surface above the undisturbed surface y=0

For the equal amplitude case ($a_1 = a_2$) and using (15), we have;

$$(60) \qquad h^{(1)} = -2a^2\cos\alpha(x\cos\theta)\left[\cos\alpha(z\sin\theta)\cos wt + \sin\alpha(z\sin\theta)\sin wt\right]$$

then

$$(61) \qquad P.E. = \tfrac{1}{2}\int_{-b}^{b}\int_{-d}^{d}\rho g(h^{(1)})^2 dz dx$$

where b and d are arbitrary limits. Since $h^{(1)}$ is the first order approximation to the surface, the potential energy is a second order quantity. Working out the integral:

$$(62) \qquad P.E. = 2a^4\rho g\left[b + \frac{\sin(2\alpha b\cos\theta)}{2\alpha\cos\theta}\right]\left[d + \frac{\sin(2\alpha d\sin\theta)}{2\alpha\sin\theta}\cos wt\right]$$

The limit of (62) as θ goes to 0 (standing wave case) is:

$$(63) \qquad \lim_{\theta\to 0} P.E. = 2a^4 d\rho g(b + \sin 2\alpha b/2)(1 + \cos 2wt)$$

and the limit of this for large b is:

$$(64) \qquad \lim_{\substack{\theta\to 0 \\ b\to\infty}} P.E. = 2a^4 db\rho g(1 + \cos 2wt)$$

The second time derivative of (64) with respect to time is proportional to the pressure variation at depth, and in this case the pressure varies with a frequency of twice that of the standing wave as it should. It is easy to see that

(65) $\lim_{\substack{\theta \to \pi/2 \\ d \to \infty}} P.E. = 4a^4 bd\rho g$

so that for the traveling wave the pressure at depth does not vary with time, which we know it shouldn't. For a general angle θ we get:

(66) $\lim_{b,d \to \infty} P.E. = 2a^4 bd\rho g$

which is also independent of time over a large area. In other words over a large area the surface for a general angle θ acts like a traveling wave and therefore causes no second order pressure variation at depth.

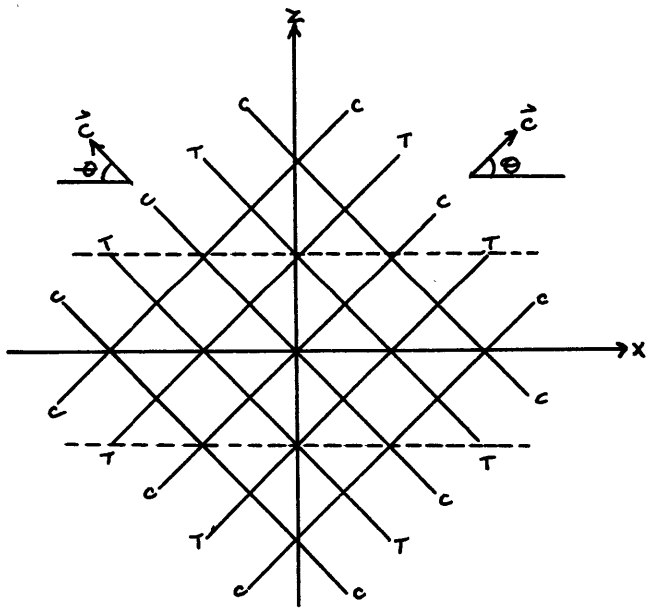

C - crest
T - trough
$\vec{c}$ - velocity

Figure 4.

In order to understand this more clearly (60) may also be written as:

(67) $\eta^{(2)} = -2a^2 \cos\alpha(x\cos\theta)\cos\alpha(z\sin\theta - ct)$

It was pointed out in Part I that this surface resembles a traveling wave in the z direction and a standing wave in the x direction. In figure 4. the solid lines represent the crests and troughs of two intersecting wave trains, and the arrows show their directions of travel. It can be seen that the pattern between the dotted lines, which has infinite extent in both directions along the x axis, moves as a unit in the z direction with a velocity $c/\sin\theta$. Thus the overall effect of the surface is that of a traveling wave, at least as far as second order effects are concerned.

It was pointed out to me by Professor Madden that in the range $\theta = 0$ to 1 degree where there exists a second order pressure at depth there might be a special direction along which especially high energy Rayliegh waves could travel. In figure 4. the surface pattern moves in the z direction with a velocity $c/\sin\theta$, where c is the water wave velocity, and for small angles this is large. If a Rayliegh wave started in a direction which made an angle γ with the z axis, and if the component of the surface pattern velocity along this direction were equal to the Rayliegh wave velocity v, then there would be strong coupling such that energy would be continuously fed into the Rayliegh wave. This special angle γ

would be given by:

$$\gamma = \arccos(c/v\sin\theta)$$

There is a smallest angle $\theta_{critical}$ for which this pnonomenon could occur, and it will be given by:

$$\theta_{critical} = \arcsin(c/v)$$

As an example, for c=15 meters/second and v=3 kilometers/second then $\theta_{critical}$ =0.3 degree and γ =0. If θ =1 degree then γ will be about 75 degrees.

Conclusion

In summary, the main problem of interest in this part is a study of what pressure variations as a function of depth exist for the case of an idealized ocean surface consisting of two infinite sine waves of the same frequency whose directions make an angle β with each other. The two simpler well known cases of a single frequency sine wave and a simple standing wave were first reviewed. The first order pressure variations of all three cases were seen to vanish with depth, and it was only in the case of a simple standing wave that there existed a second order pressure which is independent of depth and which varies with twice the frequency of the standing wave. The third case showed that for this to happen the angle β must be almost exactly 180 degrees. It is concluded, then that for the idealized models considered there exists a pressure fluctuation at the ocean floor in deep water which might cause microseisms only when two sine waves of the same frequency traveling in almost exactly opposite directions superpose at the surface. Also it may be possible in the small range β =179-180 degrees where there does exist a second order pressure fluctuation at depth for the existence of a preferred direction of travel of Rayliegh waves.

PART III

Two main investigations will be presented in this part 1) the relationship in time between the amplitudes of microseisms and water waves, and 2) the relationship between the frequencies of the microseisms and those of the water waves. These investigations are based on original data consisting of weather maps and surface weather data, and microseism and water wave records which came from the U. S. Naval Station and the Geophysical Field Station respectively in Bermuda.

The recording of the wave records will be briefly explained. Two low frequency transducers were installed off the south shore of Bermuda at the ends of a sea cable which lead ashore to amplifiers and a drum recorder. The microseism transducer was located at 32 degrees 12 minutes 24 seconds North, 64 degrees 51 minutes 39 seconds West at a depth of 165 fathoms, and the water wave one was inboard of this at a depth of 60 feet (this means that the highest frequency it could measure would be about 0.5 c.p.s.). The two signals could not be recorded simultaneously, consequently microseisms were recorded for twenty minutes, then water waves were recorded for twenty minutes etc.

The transducers were hydrophones made by Western Electric Co., and their characteristics are classified. However, the hydrophone is electrodynamic, and the response curve on the low side is 6 D.B. per octave. The amplifying system was Sanbord cardiographic D.C. amplifier modified to pperate with

a drum. The result is that only relative amplitudes are obtainable from the records, but this is enough for the purpose here. Records were available from November 2, 1952, to December 1, 1955.

The method of measuring the microseism and water wave amplitudes is similar to that used by Haq (2). The average of the four or five highest waves (crest to trough) within the first and last three minutes of each twenty minutes of record was uded to characterize the amplitude of the microseisms or water waves for that twenty minute period. Admittedly, this gives only a general picture, but a more exact one would require an absurd amount of time.

The weather maps were fairly crude and were only available once every twenty-four hours; however, most of the storms considered here occurred in the vicinity of Bermuda where surface weather information was available once every hour. Low and high areas are usually marked with an L and an H. The light closed lines are isobars and the heavier lines which cut across them are warm and cold fronts which have been indicated by a C or a W. The hurricane center is marked by what looks like two interlocking sixes at the center of a number of concentric circles. On some maps Bermuda is indicated by the letters NWD.

Four different case histories will now be presented.

Case 1) Jan. 7,8, 1954

Graph 1. indicates the amplitudes of the water waves and microseisms and maps 1a, 1b, 1c are the pertinent weather maps. From the overall appearance of graph 1. one might say that if the water wave trace were shifted to the left by about two and a half hours near 1200 G.S.T. and by about one and a half hours near 2100 G.S.T. and by about 40 minutes near 1400 G.S.T., Jan 8, then the two traces would agree pretty well. In other words it looks as if high amplitude microseisms preceeded the high amplitude water waves by much more near the beginning of the storm than near the end. By the theory that microseisms are caused by standing waves in deep water (theory 1) this would be expected if the storm were approaching Bermuda, which is what actually happened.

The weather maps show that at 1200 G.S.T. on Jan. 6 there was a cold front west of Bermuda in about the middle of map 1a, and the isobars which intersect it form fiarly sharp angles. This means that the wind on one side of the front is blowing at a fairly wide angle to the wind on the other side of the front. At 1200 G.S.T. on Jan. 7 this cold front has just passed over Bermuda, and exactly one day later it has moved some distance beyond Bermuda to the east.

The surface weather reports show that from 2430 G.S.T. to 828 G.S.T. Jan. 7 the wind on Bermuda was blowing at about N22E and increasing steadily from 13 to 26 knots. From 928 G.S.T. to 1228 G.S.T. it was blowing N45E at an average 18

knots, and from 1328 to 1828 G.S.T. it was blowing due east and its speed was increasing from 18 to 24 knots. From 1828 to 330 G.S.T. Jan 8 the wind continued to blow east at an average 22 knots, and from 0430 to 1728 G.S.T. the direction shifted to S67E and the velocity was about 24 knots.

The total overall change in direction of the wind during this time was about 90 degrees. This is a fairly wide angle, but it is nowhere near 180 degrees. It might be possible that the wind direction shifted by a larger amount somewhere out at sea and that standing waves were produced. It should be pointed out here that it was not possible to tell the direction from which the microseisms came because only one component of the ground motion was recorded. One thing is clear, however, from graph 1, and that is that it would not be possible for the microseisms to be caused by surf beating against the coast, since the amplitudes do not rise and fall simultaneously.

The first maximum in the microseism activity occurred as the cold front was passing over Bermuda when the wind was shifting direction from N45E to east, and the second maximum occurred about six hours later after the front had moved further east.

It is possible to conclude from this case that somehow the movement of the cold front caused the microseisms, perhaps by creating standing waves. It is definite, though, that the microseisms could not have been caused by surf beating on s shore.

Case 2) Feb. 22-25, 1954

The amplitudes for this case are shown on graphs 2a. and 2b., and the appropriate weather maps are maps 2a, 2b, 2c, 2d. From graph 2a. it is fairly clear that the microseisms and water wave amplitudes do not have much to do with each other, from which the conclusion is drawn that the microseisms could not have been caused by surf beating on the coast.

The first three maps show essentially the same situation as in the first case, that is a cold front moving from west to east and passing over Bermuda. Again the isobars intersect the cold front at fairly acute angles. Map 2b shows that at about 1230 G.S.T. on Feb. 23 the front has just passed over Bermuda. This correlates with the surface weather reports which show that between 930 and 1430 G.S.T. Feb 23 the wind blowing from 15 to 20 knots shifted through 110 degrees in direction from due north to S67E. The micro seisms reach a maximum about six hours after the front passed over Bermuda. This also occurred in the first case, and it shows that the maximum microseismic activity doesn't necessarily occur when the center of the storm is closest to the recording station.

In graph 2b it appears that the amplitudes reach a maximum at the same time. Actually the water wave peak occurs about 40 minutes later than the microseism peak. Three other water wave peaks seem to correlate with three microseism peaks and all three occur about 40 minutes after the corresponding microseism peaks.

Surface weather reports show that between 630 and 2230 G.S.T. on Feb 24 the wind on Bermuda was blowing from 7 to 15 knots and changed directions through 135 degrees from S45E to due north. The microseisms reach their maximum during this time at about 2100 G.S.T.. The weather maps do not show a cold front passing over Bermuda during this time, probably because they are two widely spaced. Again it is conceivable that if the wind changed direction by such a wide angle on Bermuda, it could have shifted through 180 degrees over some area at sea.

The conclusions to be reached from this case are that microseisms are not produced by surf beating on shore, but that they are probably caused by locally created standing waves.

Case 3) Sept 1-2, 1954

Graph 3. shows the amplitudes, and the pertinent weather maps are maps 3a,3b,3c. This case covers the time during which a hurricane traveling northeast passed fairly close to Bermuda on the west side. Graph 3. shows that the microseisms begin to increase and reach a maximum a little over two hours before the water waves do. The microseisms continue at about the same average level, whereas the water waves continue to increase. The usual conclusion is, then, that the microseisms could not be caused by the action of waves on the shore.

There are two high water wave peaks near 600 G.S.T., Sept. 2, which are separated by a little over four hours, and above them are two microseism peaks which are practically the same distance apart and which preceede the corresponding water wave peaks by 20-40 minutes. Also there is a third smaller peak inbetween the other two which correlates well on both curves. In Case 1) a similar feature was found.

Considering the method used to measure amplitudes, such close correlation is not really expected, only general trends are hoped to agree, and besides there are far more peaks which do not correlate between the two curves. In theory standing waves which produce microseisms could be created in such a direction that they would never be recorded by the one station. In this case the hurricane is traveling roughly in in a north-south direction, so that the standing waves it might

create would have their wave fronts approximately parallel to this direction. This means that the waves which made up the standing wave at sea would have a good chance of being recorded, since the hurricane passed by to the west of Bermuda. Perhaps, then there is a correspondence between the above mentioned set of peaks.

The hurricane on map 3a is not the main interest. It is probably the cause of the fairly high level of microseism activity at 2400 G.S.T., Sept 1 (aug. 31). One guess is that in between the time of map 3a and map 3b this hurricane traveled over land thus causing the decrease in the microseism amplitude shown at 400 G.S.T., Sept 1, on graph 3. Map 2b shows that the first hurricane has gone and another is on its way toward Bermuda. The highest microseism peak occurs before the hurricane reaches Bermuda. This may be due to the hurricane's moving faster before it reached Bermuda than after it passed, but there is no way of checking this.

The surface weather reports show that from 430, Sept 1, to 127 G.S.T., Sept 2, the wind blew N22E at 13 to 23 knots. At 227 G.S.T. the direction changed to due north and remained so for over twelve hours. During that time the wind velocity varied from 19 to 27 knots with the maximum of 27 knots at 428 G.S.T. This seems about the right time for the hurricane's closest approach to Bermuda, for it is at about this time that the water wave amplitude makes a sharp increase. The microseisms also make a slight increase in amplitude at this time,

but this is not considered significant.

The same conclusion may be made here as was made in the first two cases, namely that microseisms are not caused by wave action at the shore. One may also say that a hurricane moving over the ocean surface causes microseisms probably by creating standing waves.

Case 4) Jan 4-5, 1954

This last case is another example of a microseism storm due to the movement of a cold front. Graph 4. shows the amplitudes, and maps 4a, 4b, and 4c provide the sketchy weather data that was available. The general trend of the microseisms agrees quite well with that of the water waves, as a glance at graph 4. will show. One's first thought is that here is a case which proves that microseisms are caused by surf beating against the shore, and it is true that of the four cases examined this comes closest to verifying that hypothesis. There is one other possibility, however, and that is that the generating area for the microseisms passed quite close to Bermuda, thus producing a simultaneous increase and decrease of the water wave and microseism amplitudes. This is entirely possible since Bermuda is surrounded by deep water, whereas it does not seem to be possible along the East Coast of the United States, for example, because the storms there usually travel from land to sea, and the microseisms don't show an appreciable increase until the storm has traveled out over deep water. Thus the water waves would increase first, and the microseisms would increase at a later time. This is just what Haq observed.

The weather data gives further clues. Map 4a shows a cold front with isobars meeting it at quite sharp angles lying inland and roughly parallel to the Eastern seaboard, Twelve hours later this front has blown some distance out to sea and

is lying fairly close and to the west of Bermuda. The last map 4c shows that this cold front has passed quite some distance to the east of Bermuda, and one presumes that sometime inbetween it passed over Bermuda.

Surface weather reports indicate that at 525 G.S.T., Jan 4, the wind was blowing due north at 18 knots on Bermuda, that between 628 and 1128 G.S.T. the wind blew about N22E at an average 17 knots, and that at 1128 G.S.T. the direction changed to due east and the velocity dropped to 12 knots. Between 1229 and 1928 G.S.T. the wind direction was approximately S22E and the velocity was 10 knots on the average. At 1928 G.S.T. the direction became due south and remained so for four hours, and the velocity was 10 knots decreasing slightly during the next four hours.

During the whole fourteen hours the wind direction on Bermuda changed through exactly 180 degrees from due north to due south, and it was shortly after (perhaps 40 minutes) the wind direction changed to due south that the microsiesms reached their maximum amplitude. One might suspect from this that the generating area for the microseisms was quite close to Bermuda which would explain graph 4.; however, there is no absolute way to check this. A further clue would come from a knowledge of the frequency spectra of the microseisms and water waves, but time didn't permit this calculation.

In conclusion, the results of this case are not as definite as those of the others. In the first three cases it was

quite clear that the microseisms could not have been caused by wave action on the shore, and it was less clear but plausable that they were caused by standing waves. The plausability came from the fact that in all cases meteorological conditions existed such that at one time the wind was blowing in a certain direction over an area of ocean surface, and at a later time it blew over the same area at an obtuse angle (perhaps 180 degrees) to its earlier direction, so there is a chance that standing waves could have been created. What also adds to the plausability is that Haq (2) observed microseisms under the same meteorological conditions, and by computing a number of spectra of both water waves and microseisms, he was firmly convinced that standing waves caused the microseisms. In the last case one cannot say quite so definitely that shore breakers do not cause microseisms and therefore even less definitely that standing waves cause them. However, a fairly reasonable hypothesis, which seems to be supported by the weather data, has been suggested which would bring this case in agreement with the other three.

Frequency Relationship

The next subject to be discussed is the frequency relationship between water waves and microseisms during a storm. This section is the weakest as far as quantity of results is concerned due to the limitations of time and money; the procedure was lenghty as well as costly.

The main idea was to calculate the frequency spectra of a number of water wave and microseism records and then compare them to see if there is a two to one frequency ratio which the theory of Longuet-Higgins predicts (6). Assuming these records to be stationary time series, the method used is to first compute the autocorrelations and then take their cosine transforms to obtain the power spectra, which measure the amount of energy present at each frequency. This method is based on Norbert Wiener's generalized harmonic analysis, a detailed exposition of which may be found in references (3, 7, 8).

In computing the autocorrelations a modified version of the 'transient approximation' was used. Reference (3) gives a list of the different approximating formulas with a discussion of their various limitations. The formula used was:

$$(1) \qquad \varphi(\tau) = \sum_{i=0}^{N-\tau} f_i f_{i+\tau} \qquad \tau = 0, 1, \ldots m$$

In most cases the shift τ was only carried out to one third of the number of data points instead of the full number which

the transient approximation calls for. The transient approximation guarantees that all the power will be positive, which is desirable. However, modifying it in this way causes the guarantee not to hald any longer, but it is harmfull to shift the autocorrelation by much more than one third of the data length, because successively more and more of the data points are multiplied by zero as the shift increases. In (1) N is the total number of data points.

The cosine spectra were computed by the formula:

$$(2) \qquad \Phi(w) = \sum_{\tau>0}^{m} \varphi(\tau)\cos w_i \tau \qquad w_i = 0,\ \pi/m,\ \ldots, i\pi/m, \ldots, \pi$$

which is what J. Tukey uses except that no smoothing is used here (see reference (3) appendix m).

In order to compute equations (1) and (2) a program was written for the I.B.M. 709 at MIT, but first the data had to be put in a form which the 709 could handle. This procedure will be briefly described. First the wave records were enlarged eight times. Then they were taken to Wolf Corporation in Boston which has a Bendix G-15 computer which operates with a tracing table. As the records were traced the computer recorded the amplitude at the specified increments and punched this information on tape. In other words the records were digitalized by this process. The tapes were converted to cards by another machine at Bedford Air Base, and then these cards were converted to a form which the 709 could use

by a program written by Professor Simpson.

The main program used to compute (1) and (2), which is given in the appendix, was basically designed to compute the autocorrelation using all the digitalized data, and then to compute its cosine transform for a discrete set of frequencies with arccosines between zero and 180 degrees; the frequency spacing was usually 1/120 c.p.s. A certain amount of flexability was incorporated into the program in order to be able to vary the following quantities: the maximum shift in the autocorrelation, the number of data points used in the autocorrelation, and the highest desired frequency in the cosine transform. The number of data points used was varied by selecting every n^{th} point of the original digitalized data before the autocorrelation is computed, and this produces the same effect as if the original record had been digitalized at 1/n times the original rate (where n=1,2,3,...). The cosine transforms of the 'thinned' data (same time length but fewer data points) are then computed using the same frequencies starting from zero, but now the maximum allowable frequency is smaller, because the highest frequency one could hope to get has one wave length equal to the distance between two adjacent points in the autocorrelation, and the number of points in the autocorrelation is now smaller. If one computes beyond the highest allowable frequency one will obtain a mirror image of the original spectrum where the mirror is located at this highest allowable frequency. This is not

harmful, but for the purposes here it is a waste of computer time.

The four records which were run through the 709 were taken from Case 2) in the vicinity of 1900 G.S.T., Feb. 23, 1954, during which time the most intense period of that particular microseismic storm was occuring. The records in order of occurrence are: record 1) at 1840 G.S.T. (water wave), record 2) at 1900 G.S.T. (microseism), record 3) at 1920 G.S.T. (water wave), and record 4) at 2000 G.S.T. (water wave). The original records are shown in plate 1. along with a number of others which were not digitalized. From looking at plate 1. one can see just by eye that in a number of places the period of the water waves is twice that of the microseisms. In plate 1. every other trace is a microseism recording with the water wave recordings inbetween; the darker noisier looking traces are the microseisms. The total length of record shown is approximately three minutes; the tic marks are spaced one minute apart. Plate 2. shows the digitalized product of record 1). All four records were three minutes in length; the microseism record was digitalized at the rate of 512 points per minute, and the three water wave records were digitalized at half that rate, i.e. 256 points per minute of record.

The results of the autocorrelation and its cosine transform for record 1) are shown in graph 5. The autocorrelation appears extremely periodic, and it is obvious that three minutes of record was not sufficient to make it die to zero.

Corresponding to this period in the autocorrelation there is a sharp spike in the power spectrum at 0.141 ± 0.004 c.p.s. In this case the spectrum was computed out to the highest possible frequency, and after 0.25 c.p.s. the curve oscillates about a constant low level. Remember energy is not expected for frequencies greater than about 0.5 c.p.s. due to the fact that the water wave transducer was under 60 feet of water.

The results for the microseisms (record 2)* are shown in graph 6. The autocorrelation again appears very periodic and shows a beat phonomenon as well; the beat phonomenon will be discussed later. The spectrum is more complicated, and the major peaks occur at 0.25± 0.007, 0.275 ± 0.007, 0.300 ± 0.007, 0.338 ± 0.007, and 0.375 ± 0.007 c.p.s.; the one at 0.300 c.p.s. has the most energy associated with it. The peak which is most nearly equal to twice the peak of record 1) is the second one, and these two peaks satisfy the two to one ratio within the resolution limits of the two spectra.

The peak of interest in the spectrum of water wave record 3) occurs at 0.133 ± 0.004 c.p.s., and twice this frequency just barely agrees with the first major peak in the microseism spectrum. Graph 7. also shows a fairly large amount of energy associated with extremely low frequencies. This seams reasonable from looking at the autocorrelation, but other than that an explanation for it is lacking.

The spectrum of water wave record 4) (graph 8.) has

* This spectrum is suspected of being wrong

most of its energy concentrated at 0.117 ± 0.004 c.p.s., and there is really no peak in the microseism spectrum which is twice this value. It is also curious that none of the water wave peaks correspond to twice the largest peak of the microseism spectrum. However an idea of just how constant the water wave frequencies are during a microseismic storm can be seen from the results of the three water wave spectra. During the hour and twenty minutes under consideration, the water wave peaks varied from 0.141 ± 0.004 to 0.117 ± 0.004 c.p.s. The fact that they decrease with time is not considered significant. The conjecture is that somewhere inbetween the three minute sections sampled the frequency peak in the water wave spectrum could easily have attained a value, which when doubled would match the highest microseism peak, without varying by more than it did during the hour and twenty minute period.

Further unexpected results were obtained in connection with the beat phonomenon mentioned above. In the microseism autocorrelation (graph 6.) beats occur with an average period of 40.0 seconds; the highest and lowest numbers in this average are about 35 and 50 seconds. This means that the highest peak in the spectrum should be split into two frequencies with a frequency spread given by $f=1/4T$, where T is the beat period), which is 6.25×10^{-3} c.p.s. The resolving power of the spectrum is only 1.25×10^{-2} c.p.s. which is not enough to show the split. What may be an amazing coincidence is that in

wave record 4) (graph 8.) beats also occur with a half period of about 50 seconds. Also in graph 10., in which the autocorrelation of wave record 1) was shifted 2/3, a hint of beats is present with a half period of about 50 seconds. In other words, the period of the beats in the water wave autocorrelation and the period of the beats in the microseism autocorrelation roughly satisfy the two to one relationship which Longuet-Higgins would predict in this case, assuming that the problem is linear.

Another result was obtained which has more computational interest than direct bearing on the main problem. Autocorrelations were computed for water wave record 1) selecting every point of the digitalized data, every second, third, fifth, and tenth point. The power spectra were then computed, and the results are shown in graphs 5. and 8. It will be noticed that the highest spike occurs at the same frequency in all cases; in fact, the general appearance of the spectrum is practically the same in all cases. This means that the record could just as easily have been digitalized at 1/10 times the original rate, i.e. 25 points per minute of record, and the same results would have been obtained. It will be noticed that the relative height of the spike to the background level decreases with fewer data points used; an explanation for this is lacking.

Conclusions

In conclusion, it has been found in the first three case histories that the theory that microseisms are caused by the surf beating against the shore cannot be correct, but that the theory that microseisms are caused by standing waves on the ocean surface is very likely the right one. The results of Case 4) are not so definite, but a plausable hypothesis is presented which would enable these results to agree with those of the first three cases.

From the frequency analysis of four records (three water wave and one microseism) selected from Case 2) we have seen that the two to one frequency relationship, which must hold if the standing wave theory of microseisms is true, was verified by two out of the three water wave records within the accuracy of the method. The phonomenon of beats which occurred in the autocorrelation of the microsiesm record and in at least one water wave autocorrelation show a rough two to one ratio in their respective periods.

Lastly, of computational interest is the result that reliable spectra were obtained when the record was digitalized at as low a rate as 30 points per cycle of the desired frequency, which seems reasonable because 30 is still quite a large number.

BIBLIOGRAPHY

1. Davenport, Wilbur B. and Root, William L., An Introduction to the Theory of Random Signals and Noise. New York: Mc Graw-Hill Book Company, Inc., 1958.

2. Haq, Kazi E., The Nature and Origin of Microseisms. Ph.D. Thesis, Department of Geology and Geophysics, June, 1954.

3. Hurley, P. M., Wadsworth, G. P., and Bryan, J. G., The Interrelation of the Deterministic and Probabilistic Approaches to Seismic Problems, MIT GAG Report No. 11, 1957.

4. Lamb, Horace, Hydrodynamics. New York: Dover Publications, 1945.

5. Lee, Y. W., Statistical Theory of Communication. New York: John Wiley & Sons, Inc., 1960.

6. Longuet-Higgins, M. S.,A Theory of the Origin of Microseisms. Phil. Trans. Roy. Soc. London (A), 1950.

7. Stoker, J. J., Water Waves. New York: Interscience Publishers, Inc., 1957.

8. Wadsworth, G. P., Robinson, E. A., Bryan, J. G., and Hurley, P. M., Detection of Reflections on Seismic Records by Linear Operators. Geophysics, 1953.

9. Wiener, Norbert, Extrapolation, Interpolation, and Smoothing of Stationary Time Series. New York: John Wiley & Sons, Inc.

APPENDIX

Fortran Program for the I.B.M. 709 Used to Calculate Autocorrelations and Their Cosine Transforms.

```
      XEQ
      LIST
      READ INPUT TAPE 4,5,MMM                 no. of data decks
    5 FORMAT(1I6)
      DO 17 LL=1,MMM
      READ INPUT TAPE 4,4,KKK                 min. no. of data
    4 FORMAT(1I6)                             points selected
      READ INPUT TAPE 4,6,JJJ                 max. no. of data
    6 FORMAT(1I6)                             points selected
      READ INPUT TAPE 4,3,M                   max. shift of
    3 FORMAT(1I6)                             autocorrelation
      READ INPUT TAPE 4,2,JJ                  max. frequency
    2 FORMAT(1I6)                             computed
      DIMENSION D(100000),ACOR(3500),CT(3500)
      READ INPUT TAPE 4,8,N                   total no. of data
    8 FORMAT(1I6)                             points
      READ INPUT TAPE 4,9,(D(I),I=1,N)        data
    9 FORMAT(10F7.0)
      CALL REMAV(N,D)                         mean removing
      CALL BRITER                             subroutine
      CALL SCID(5H1459)                       writes 1459 on film
      CALL FRAME                              advances film
      DO 17 LM=KKK,JJJ                        loop on no. of data
      DO 12 IT=1,M,LM                         points
      ACOR(IT)=0.                             loop on shift
      MM=N-IT+1
      DO 11 I=1,MM,LM                         loop on products
      J=IT+I-1
      ACOR(IT)=D(I)*D(J)+ACOR(IT)
   11 CONTINUE
```

READS IN DATA AND CONSTANTS

COMPUTES AUTOCORRELATION

```
      X=-1.+FLOATF(IT)*2./FLOATF(M)          plots autocor. on
      Y=ACOR(IT)/ACOR(1)                     scope point by
      CALL SCOPE(X,Y)                        point and normal-
      CALL SCOPE(X,0)                        ized to max.
                                             plots axis
   12 CONTINUE
      CALL FRAME                             advances film
      WRITE OUTPUT TAPE 2,26,(ACOR(IT),IT=1,M,LM) prints
   26 FORMAT(17H AUTOCORRELATION/(6E18.8))        out
      P=((M-1)/LM)                           autocor.
      R=3.1416/P
      DO 20 K=1,JJ                           loop on freq.
      S=K
      W=(S-1.)*R
      CT(K)=0.
      DO 14 IT=1,M,LM                        loop on products
      T=(IT-1)/LM
      CT(K)=ACOR(IT)*COSF(T*W)+CT(K)
   14 CONTINUE
   20 CONTINUE
      BIG=0.                                 finds max. in
      DO 15 I=1,JJ                           spectrum
      BIG=MAXIF(BIG,CT(I))
   15 CONTINUE
      DO 21 K=1,JJ,LM                        plots spectrum
      XX=-1.+FLOATF(K)*2./FLOATF(JJ)         normalized to max.
      YY=CT(K)/BIG
      CALL SCOPE(XX,YY)
      CALL SCOPE(XX,0)                       plots axis
   21 CONTINUE
      CALL FRAME                             advances film
      WRITE OUTPUT TAPE 2,25,M,JJ,R,W,(CT(I),I=1,JJ)
   25 FORMAT(3H M=,I5/4H NW=,I5/4H LW=,E18.8/
     4H HW=,E18.8/17H COSINE TRANSFORM/(6E18.8)) writes
   17 CONTINUE                                   out
      CALL EXIT                              cosine transform
      END
```

COMPUTES COSINE TRANSFORM

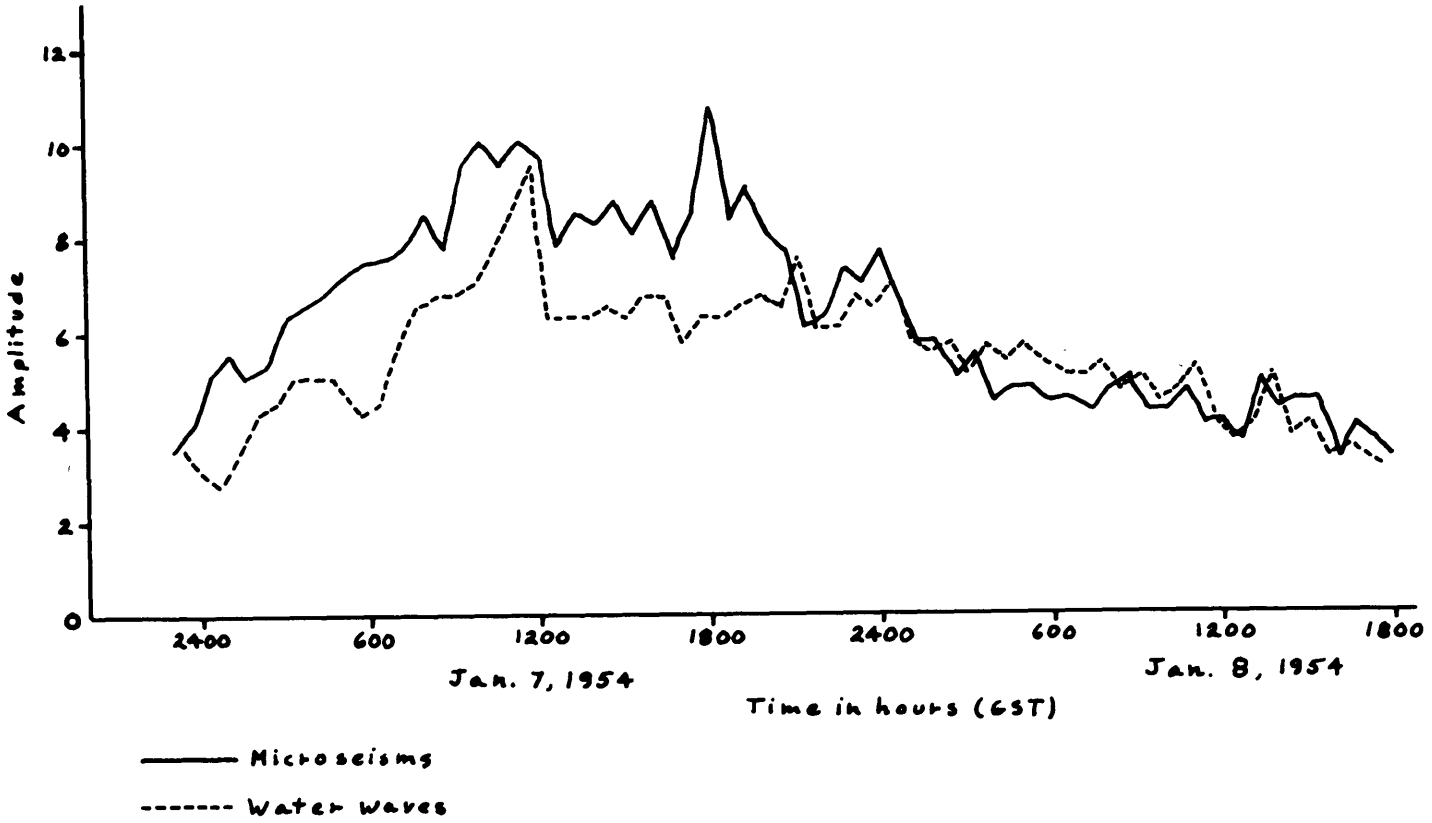
Amplitude
0
2
4
6
8
10
12
2400
600
1200
1800
2400
600
1200
1800
Jan. 7, 1954
Jan. 8, 1954
Time in hours (GST)
Microseisms
Water waves

Graph 1.

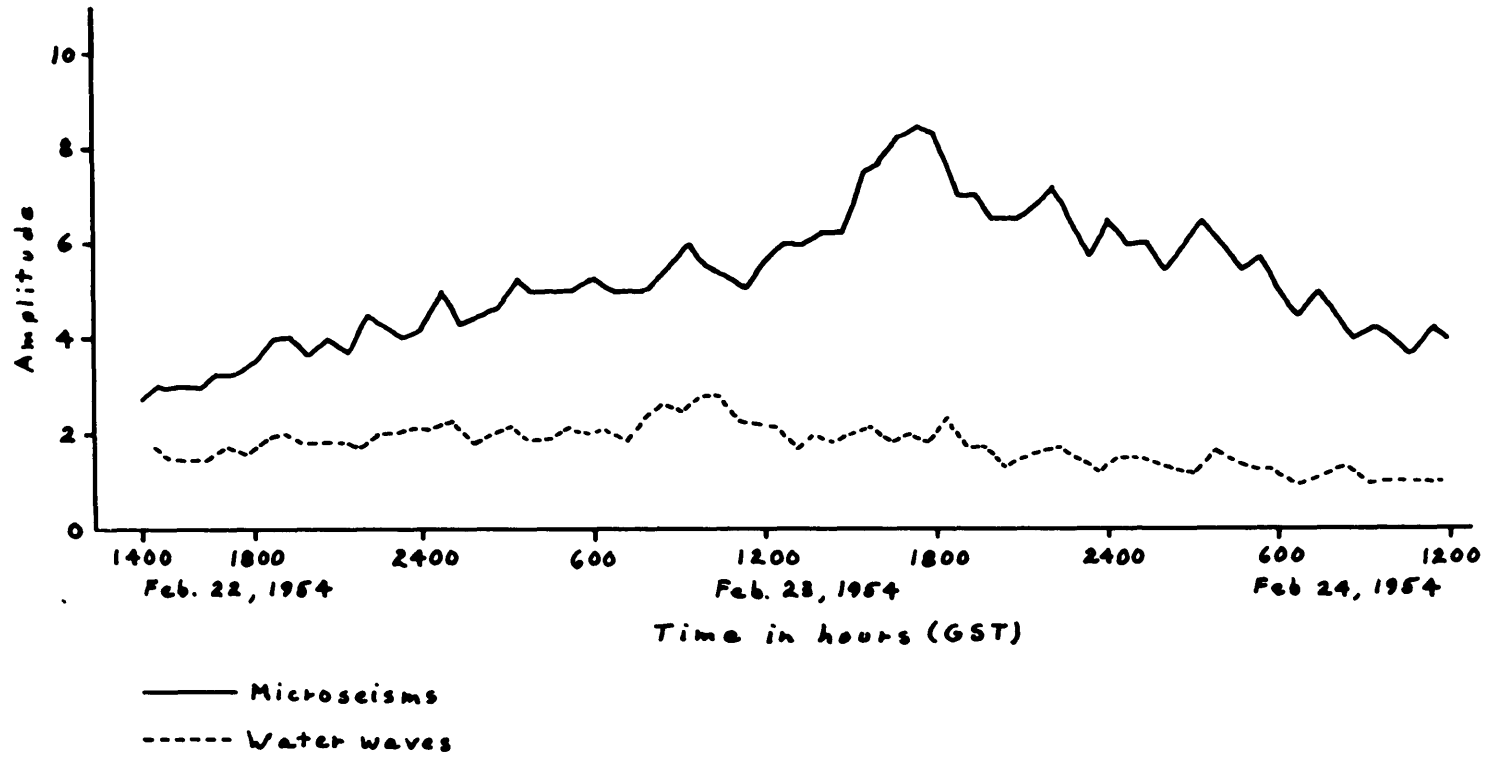
Amplitude
10
8
6
4
2
0
1400
1800
2400
600
1200
1800
2400
600
1200
Feb. 22, 1954
Feb. 23, 1954
Feb 24, 1954
Time in hours (GST)
Microseisms
Water waves

Graph 2a.

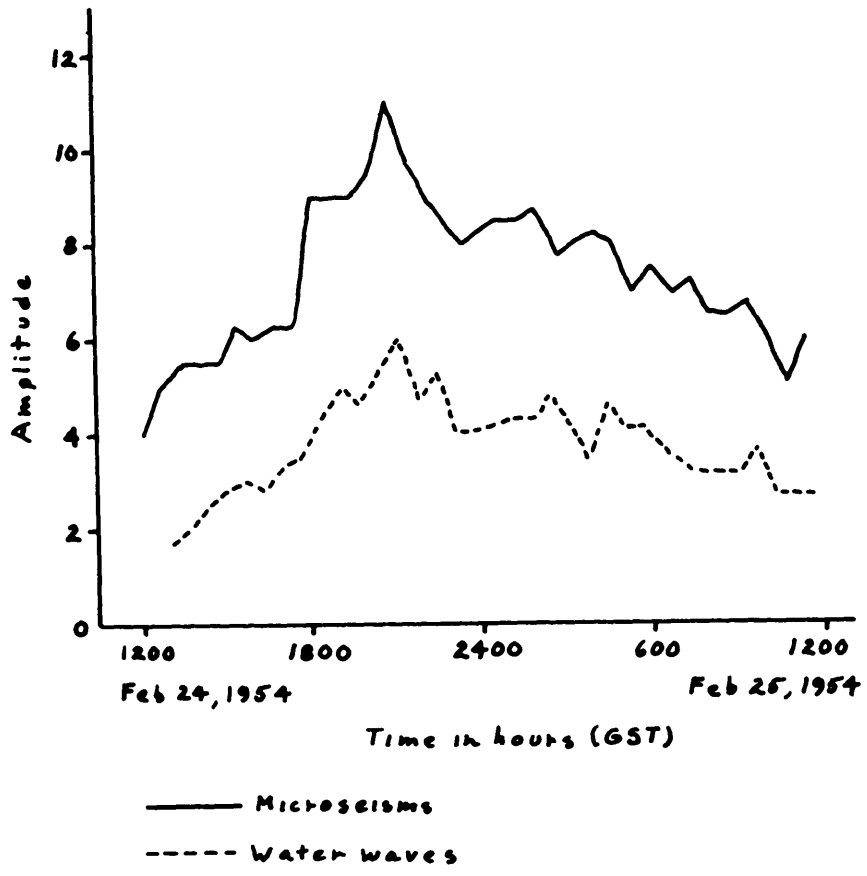
Amplitude
12
10
8
6
4
2
0
1200
1800
2400
600
1200
Feb 24, 1954
Feb 25, 1954
Time in hours (GST)
Microseisms
Water waves

Graph 2b.

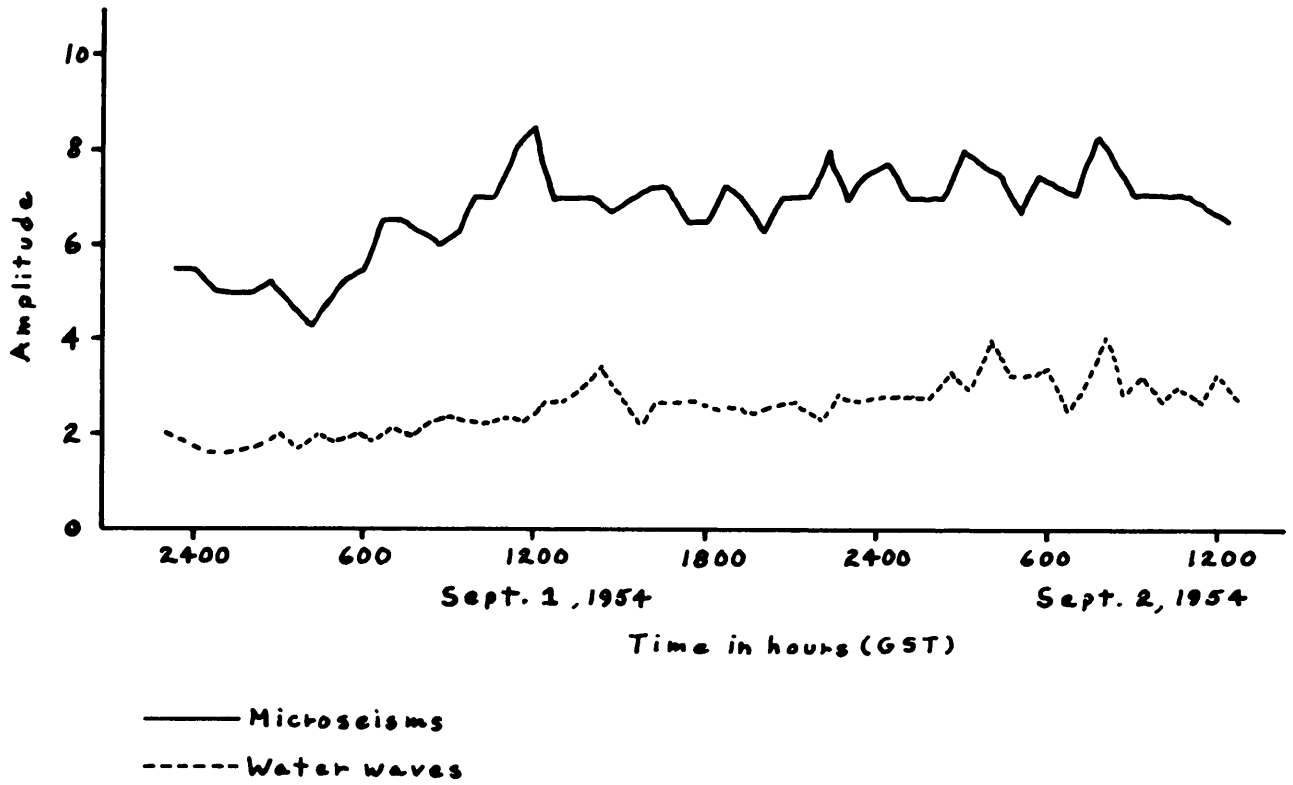
10
8
6
4
2
0
Amplitude
2400
600
1200
1800
2400
600
1200
Sept. 1, 1954
Sept. 2, 1954
Time in hours (GST)
Microseisms
Water waves

Graph 3.

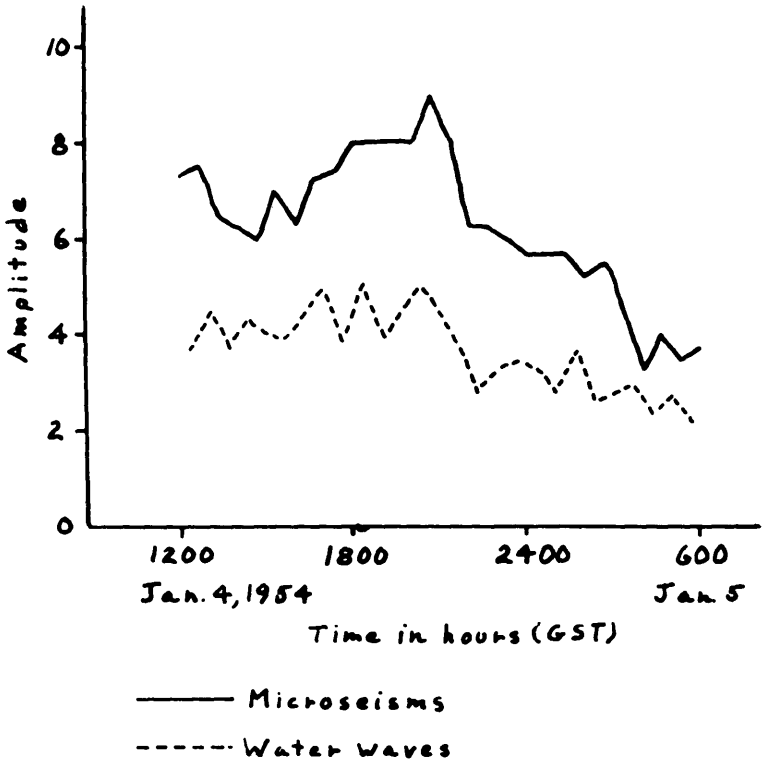
10
8
6
4
2
0
Amplitude
1200
1800
2400
600
Jan. 4, 1954
Jan 5
Time in hours (GST)
Microseisms
Water waves

Graph 4.

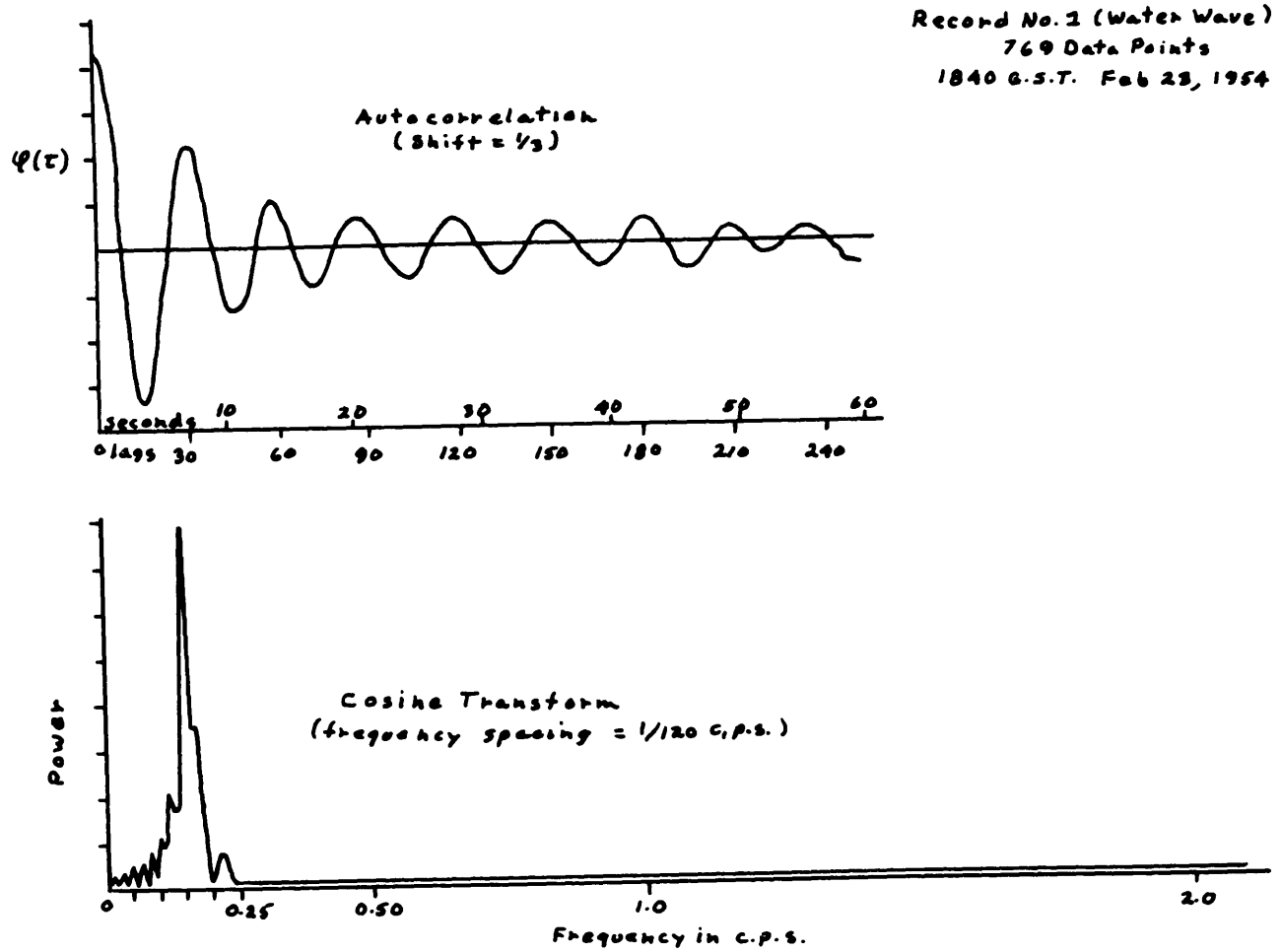
Record No. 1 (Water Wave)
769 Data Points
1840 G.S.T. Feb 23, 1954
Autocorrelation
(Shift = 1/3)
φ(τ)
seconds 10 20 30 40 50 60
0 lags 30 60 90 120 150 180 210 240
Cosine Transform
(frequency spacing = 1/120 c.p.s.)
Power
0 0.25 0.50 1.0 2.0
Frequency in c.p.s.

Graph 5.

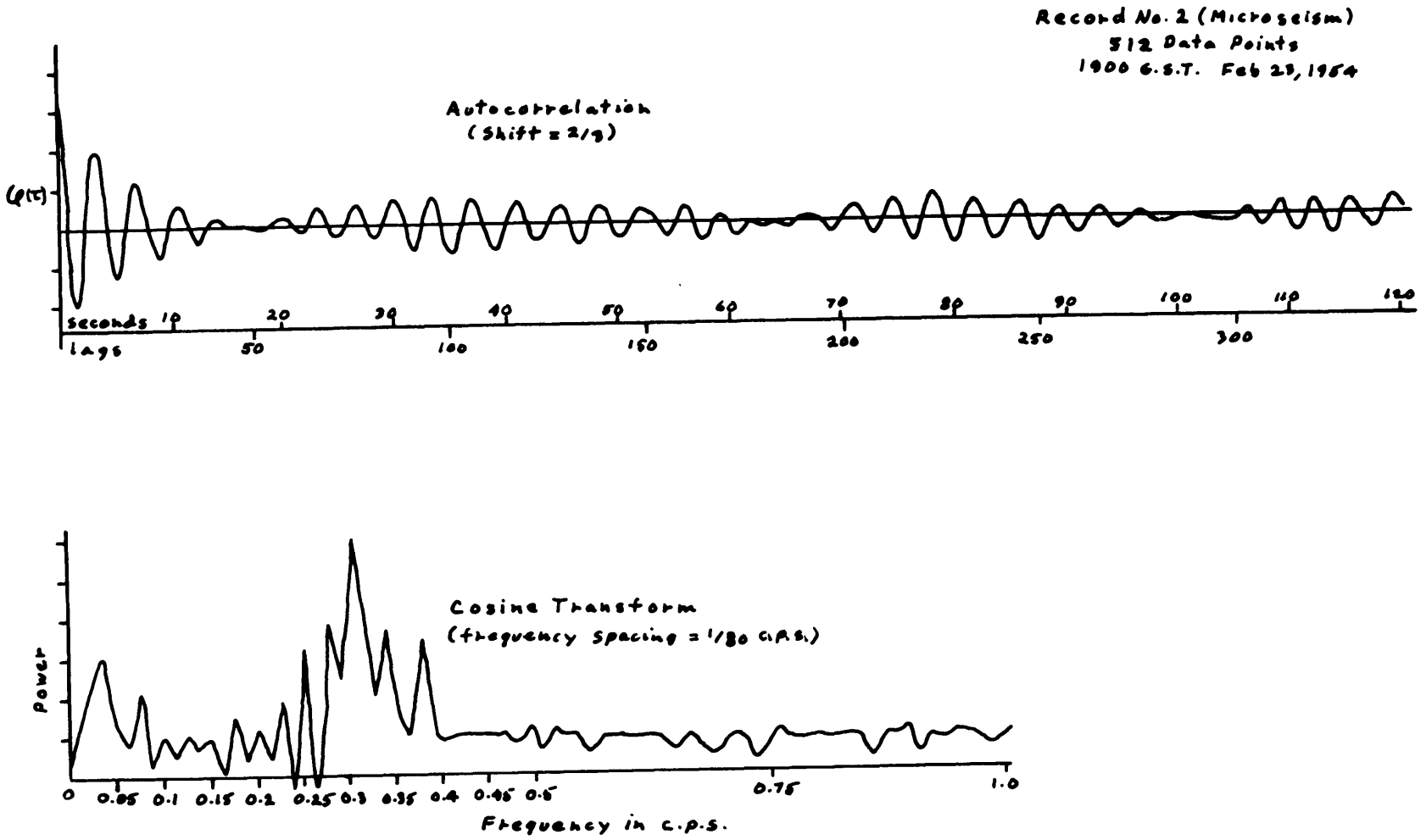
Record No. 2 (Microseism)
512 Data Points
1900 G.S.T. Feb 23, 1954
Autocorrelation
(Shift = 2/3)
φ(τ)
seconds 10 20 30 40 50 60 70 80 90 100 110 120
lags 50 100 150 200 250 300
Power
Cosine Transform
(frequency spacing = 1/80 C.P.S.)
0 0.05 0.1 0.15 0.2 0.25 0.3 0.35 0.4 0.45 0.5 0.75 1.0
Frequency in c.p.s.

Graph 6.

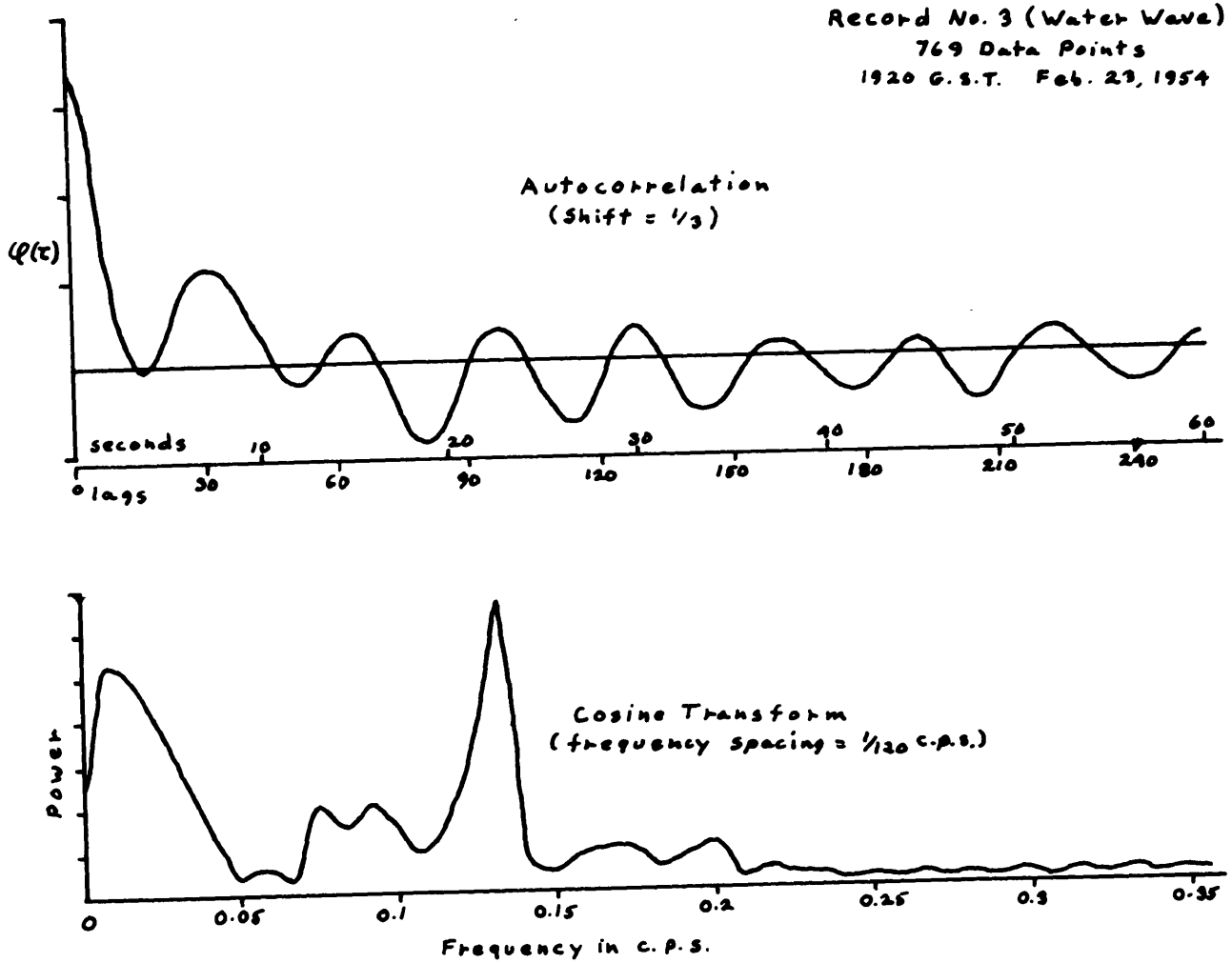
Record No. 3 (Water Wave)
769 Data Points
1920 G.S.T. Feb. 23, 1954
Autocorrelation
(Shift = 1/3)
φ(τ)
seconds
10
20
30
40
50
60
0 lags
30
60
90
120
150
180
210
240
Power
Cosine Transform
(frequency spacing = 1/120 c.p.s.)
0
0.05
0.1
0.15
0.2
0.25
0.3
0.35
Frequency in c.p.s.

Graph 7.

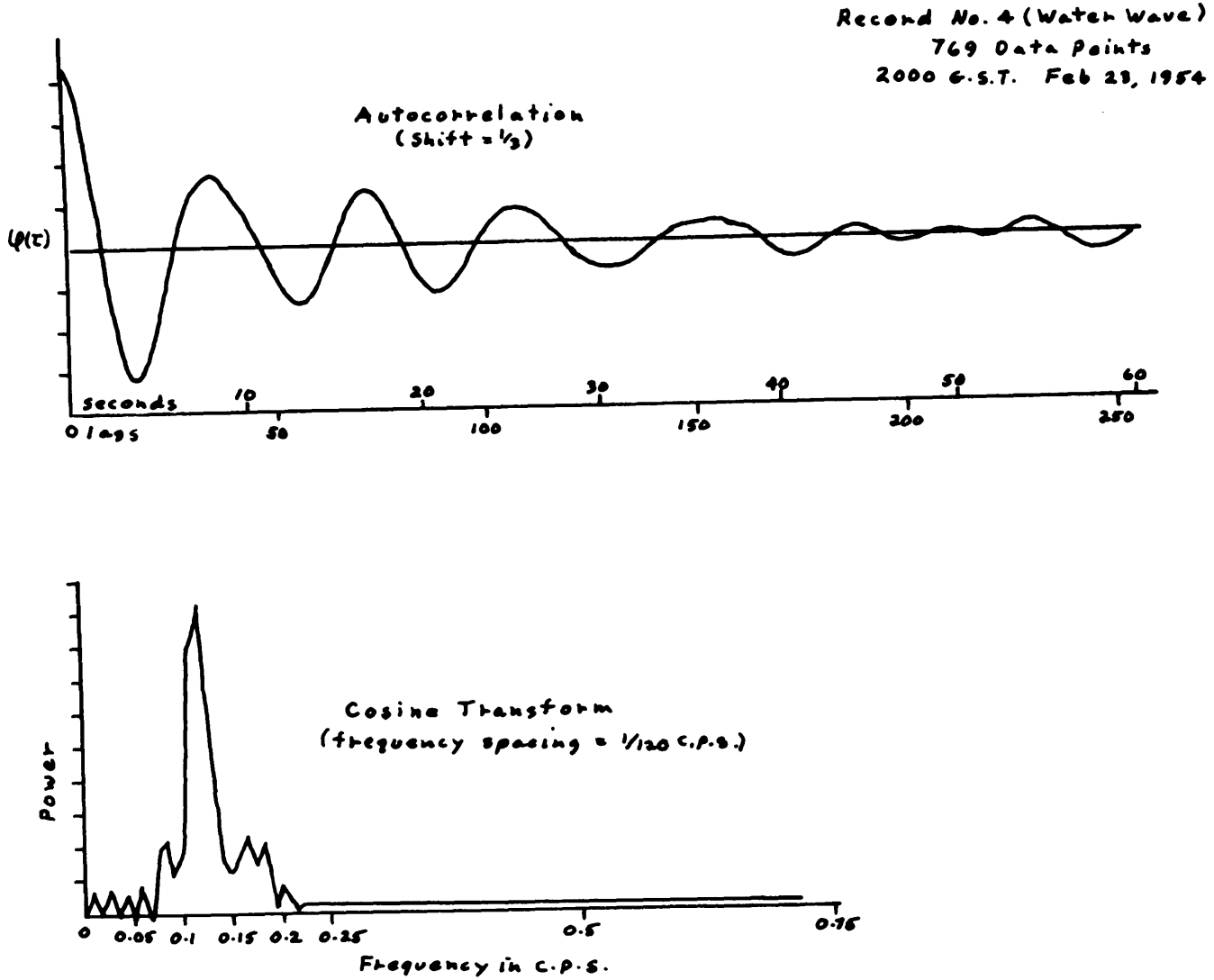
Record No. 4 (Water Wave)
769 Data points
2000 G.S.T. Feb 23, 1954
Autocorrelation
(Shift = 1/3)
φ(τ)
seconds
10
20
30
40
50
60
0 lags
50
100
150
200
250
Power
Cosine Transform
(frequency spacing = 1/120 c.p.s.)
0
0.05
0.1
0.15
0.2
0.25
0.5
0.75
Frequency in c.p.s.

Graph 8.

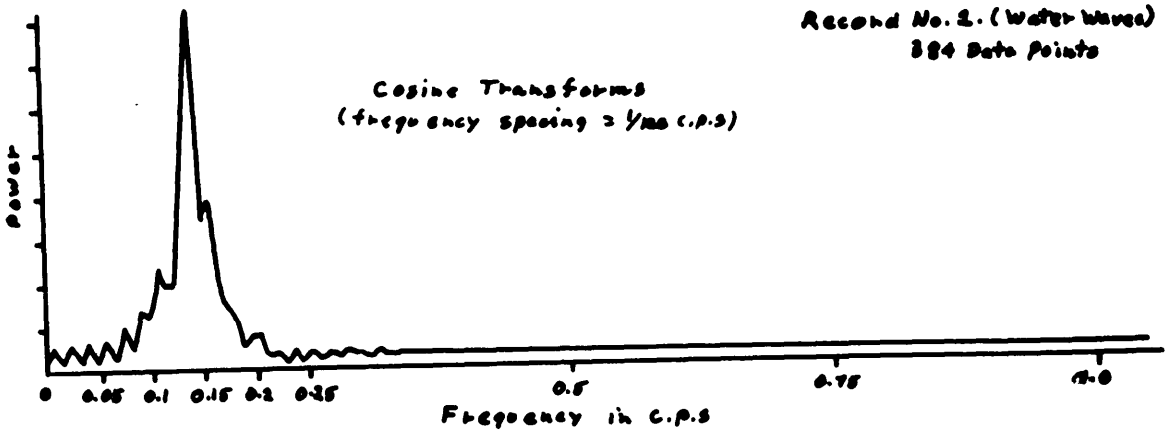
Record No. 2. (Water Waves)
384 Data Points
Cosine Transforms
(frequency spacing = 1/384 c.p.s)
Power
0
0.05
0.1
0.15
0.2
0.25
0.5
0.75
1.0
Frequency in c.p.s

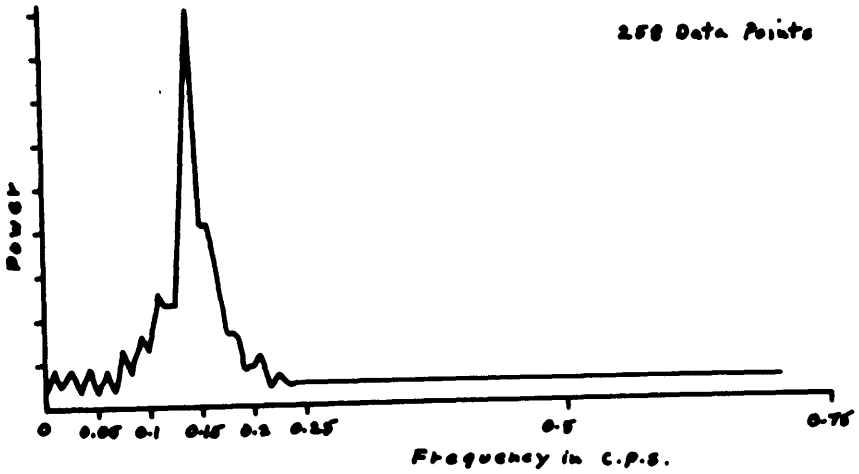
256 Data Points
Power
0
0.05
0.1
0.15
0.2
0.25
0.5
0.75
Frequency in c.p.s.

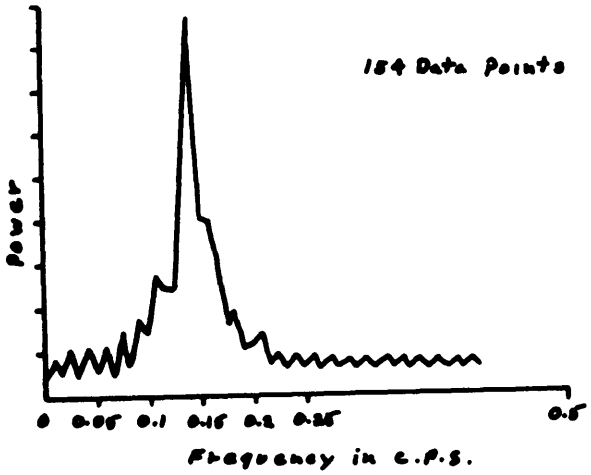
128 Data Points
Power
0
0.05
0.1
0.15
0.2
0.25
0.5
Frequency in c.p.s.

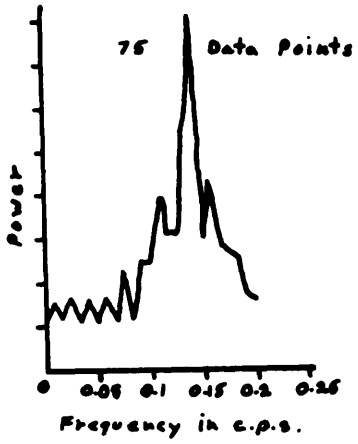
75 Data Points
Power
0
0.05
0.1
0.15
0.2
0.25
Frequency in c.p.s.

Graph 9.

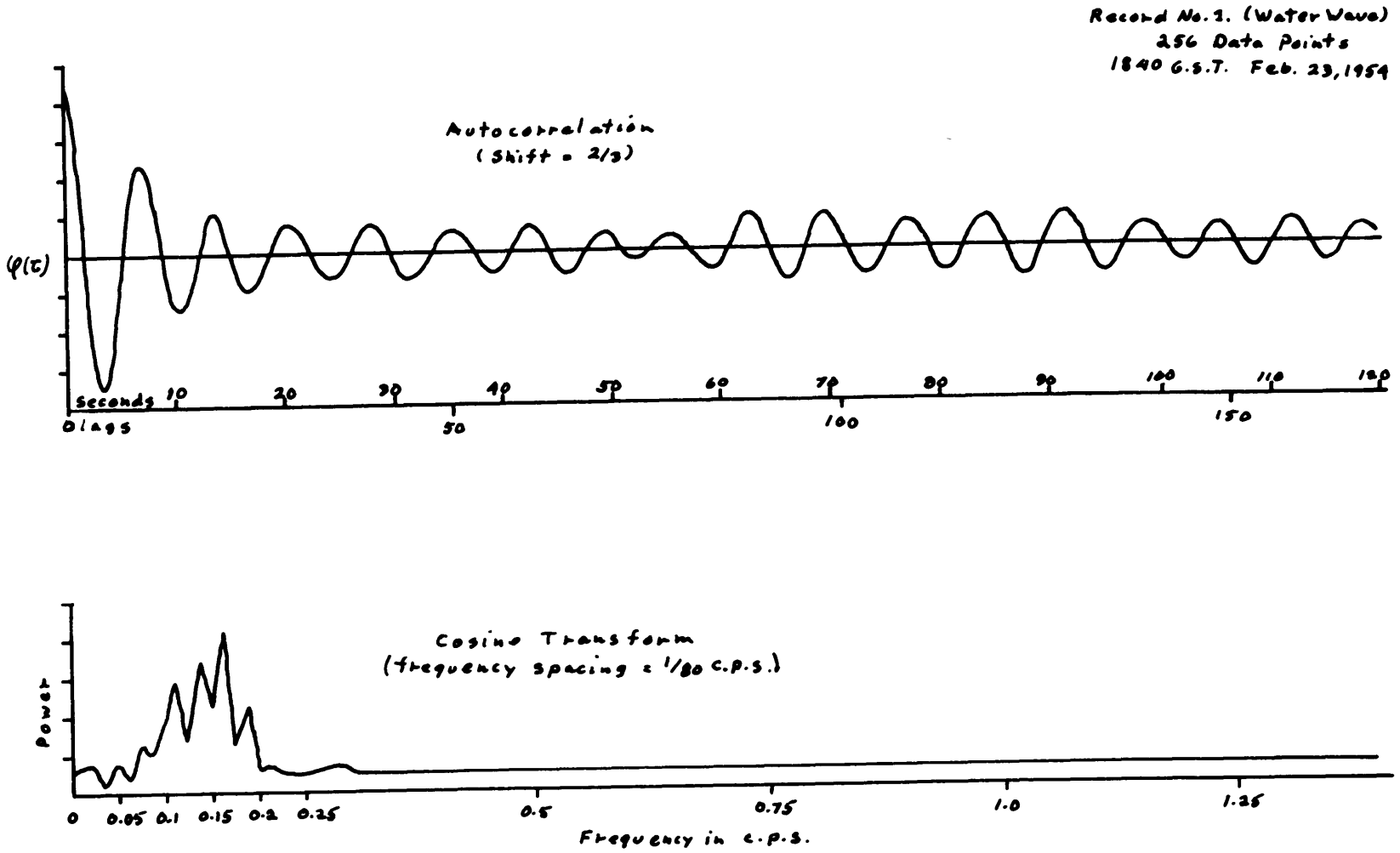
Record No. 1. (Water Wave)
256 Data Points
1840 G.S.T. Feb. 23, 1954
Autocorrelation
(Shift = 2/3)
φ(τ)
Seconds 10 20 30 40 50 60 70 80 90 100 110 120
0 lags 50 100 150
Cosine Transform
(frequency spacing = 1/80 c.p.s.)
Power
0 0.05 0.1 0.15 0.2 0.25 0.5 0.75 1.0 1.25
Frequency in c.p.s.

Graph 10.

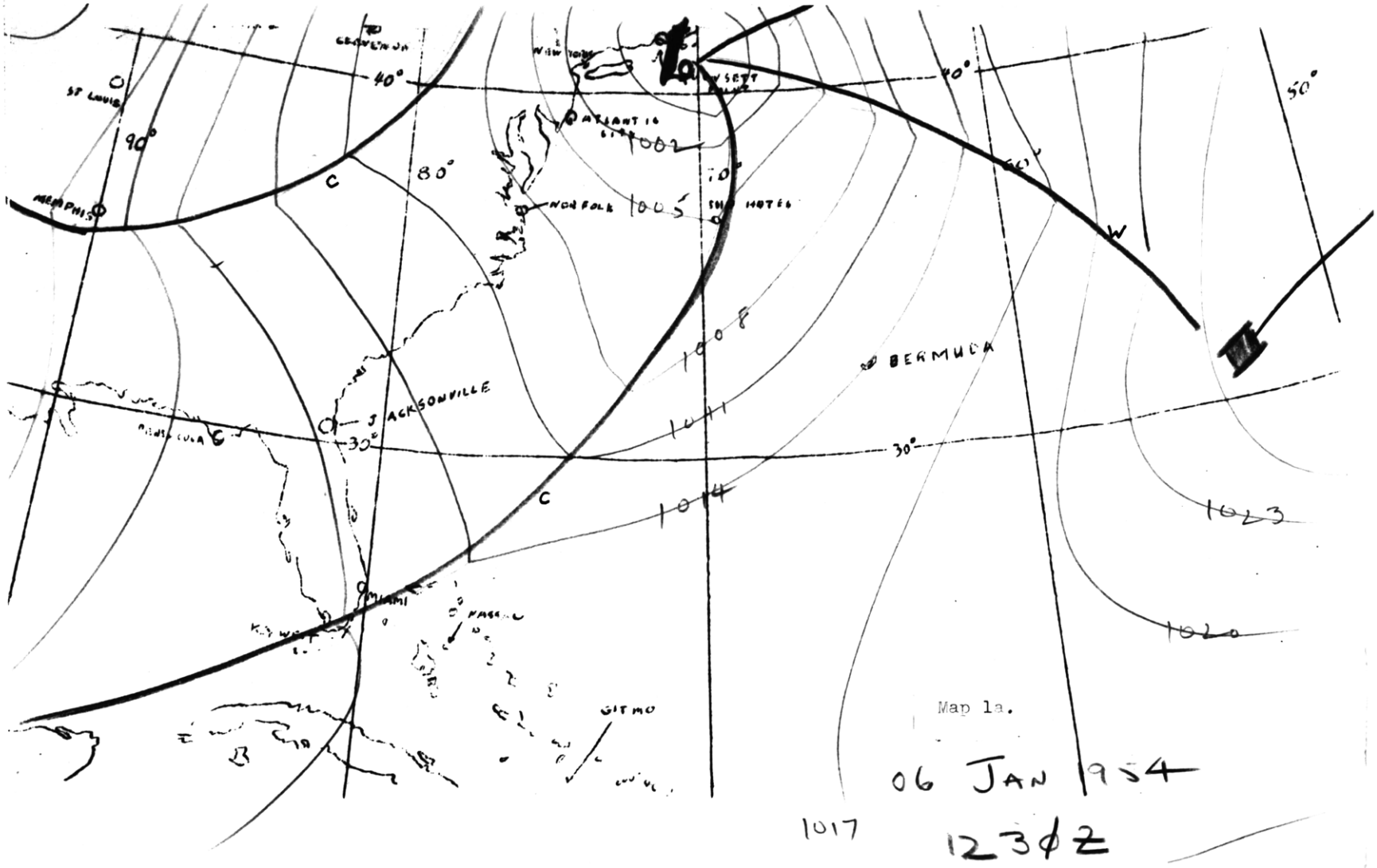

Map 1a.

06 JAN 1954

1230Z

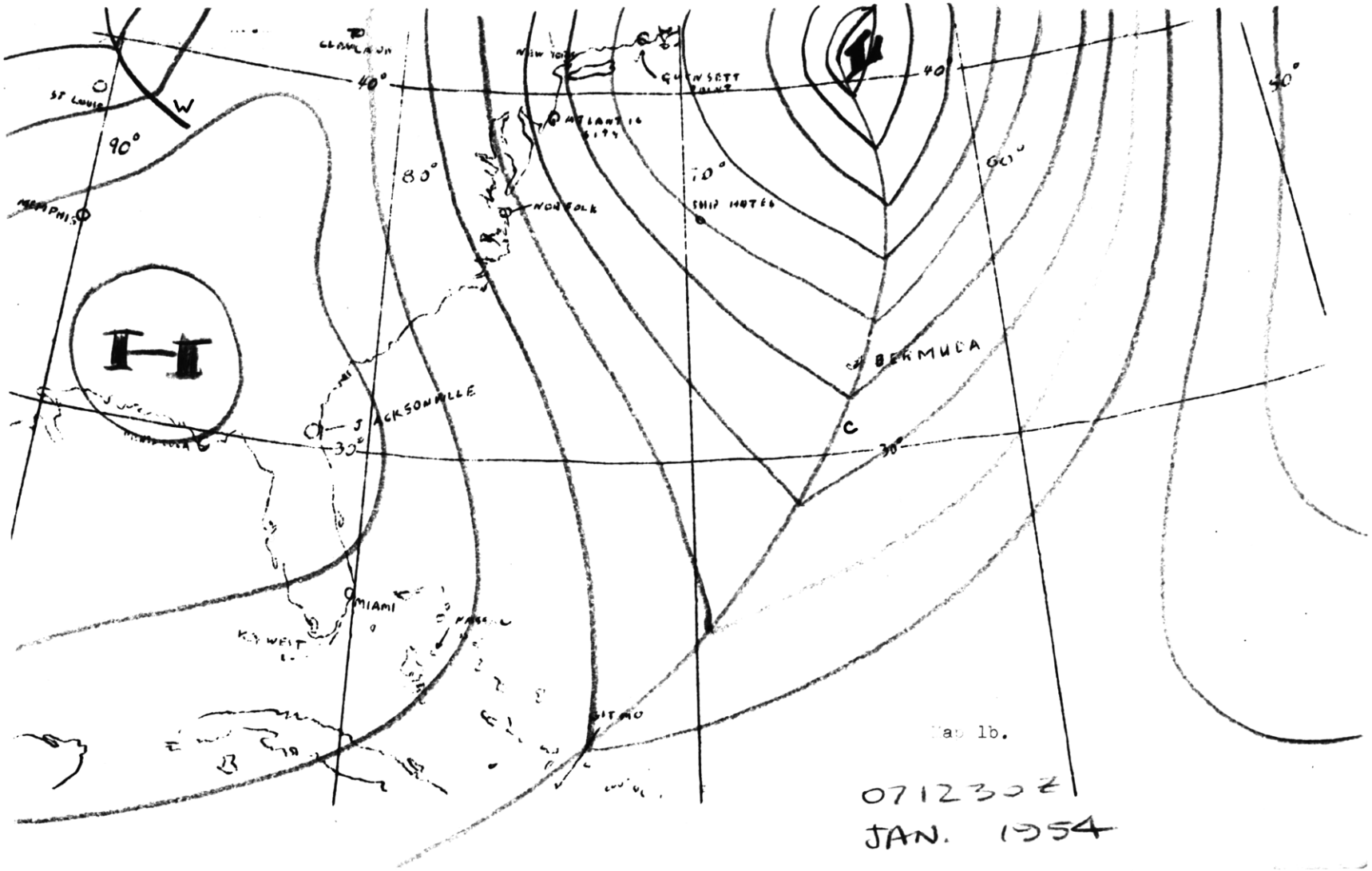

Fig. 1b.

071230Z
JAN. 1954

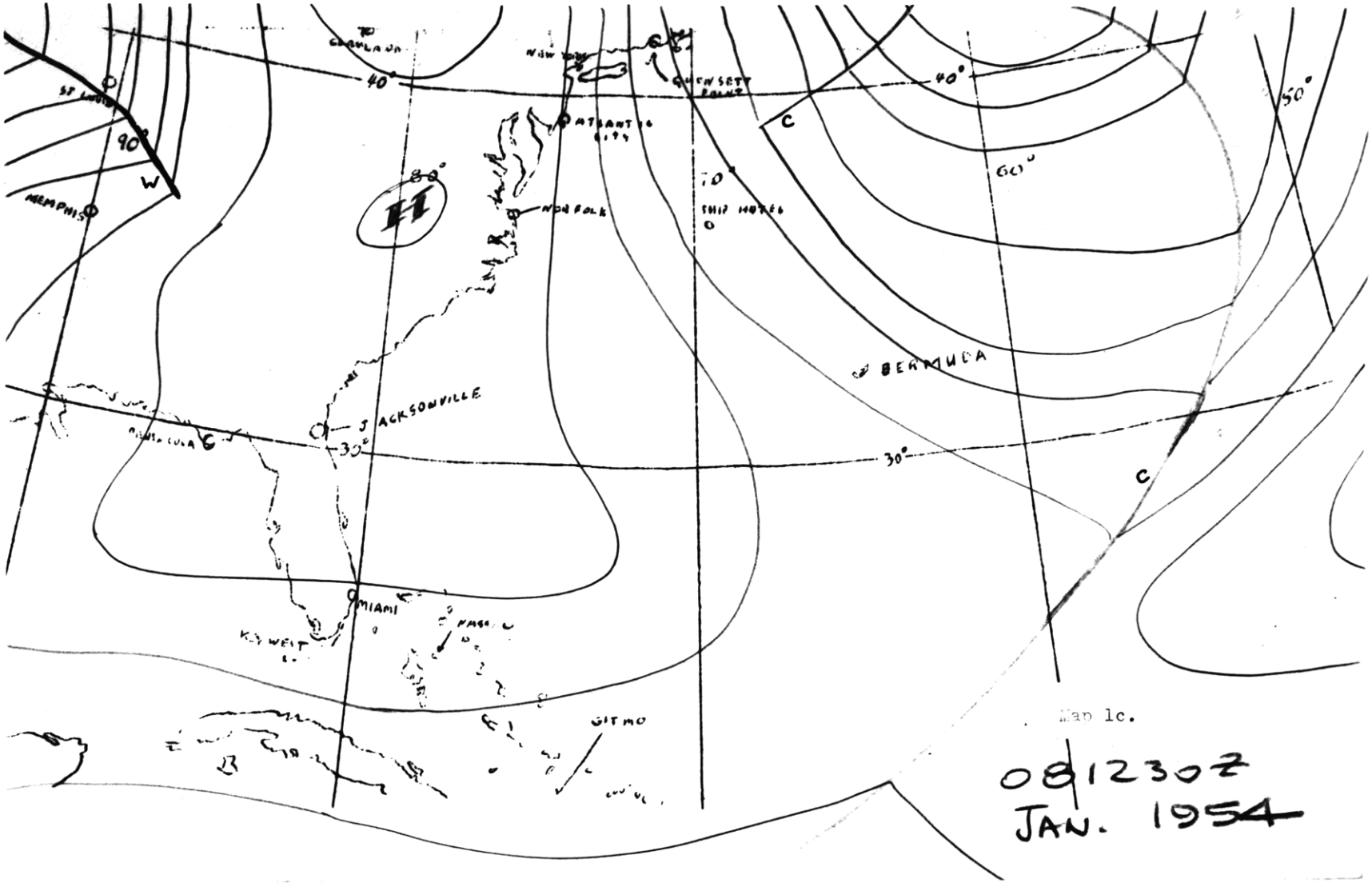
40°
90°
W
MEMPHIS
H
80°
NORFOLK
70°
SHIP HOTEL
40°
50°
60°
C
BERMUDA
JACKSONVILLE
30°
MIAMI
KEY WEST
GITMO
Map 1c.
08/1230Z
JAN. 1954

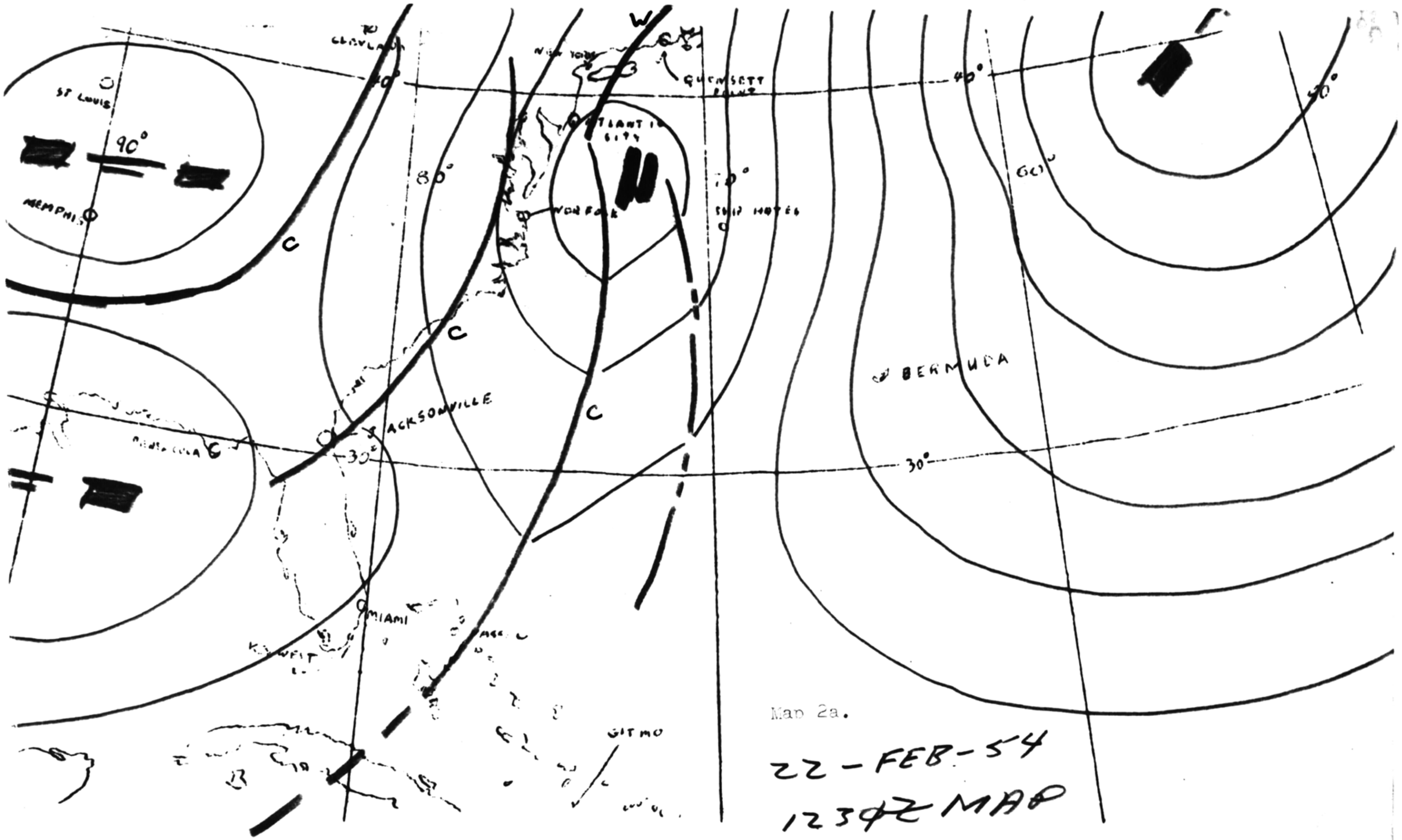
CLEVELAND
NEW YORK
QUONSETT POINT
ST LOUIS
90°
MEMPHIS
80°
NORFOLK
ATLANTIC CITY
70°
SHIP HOTEL
60°
40°
50°
BERMUDA
JACKSONVILLE
PENSACOLA
30°
MIAMI
NASSAU
KEY WEST
GITMO
Map 2a.
22-FEB-54
1230Z MAP

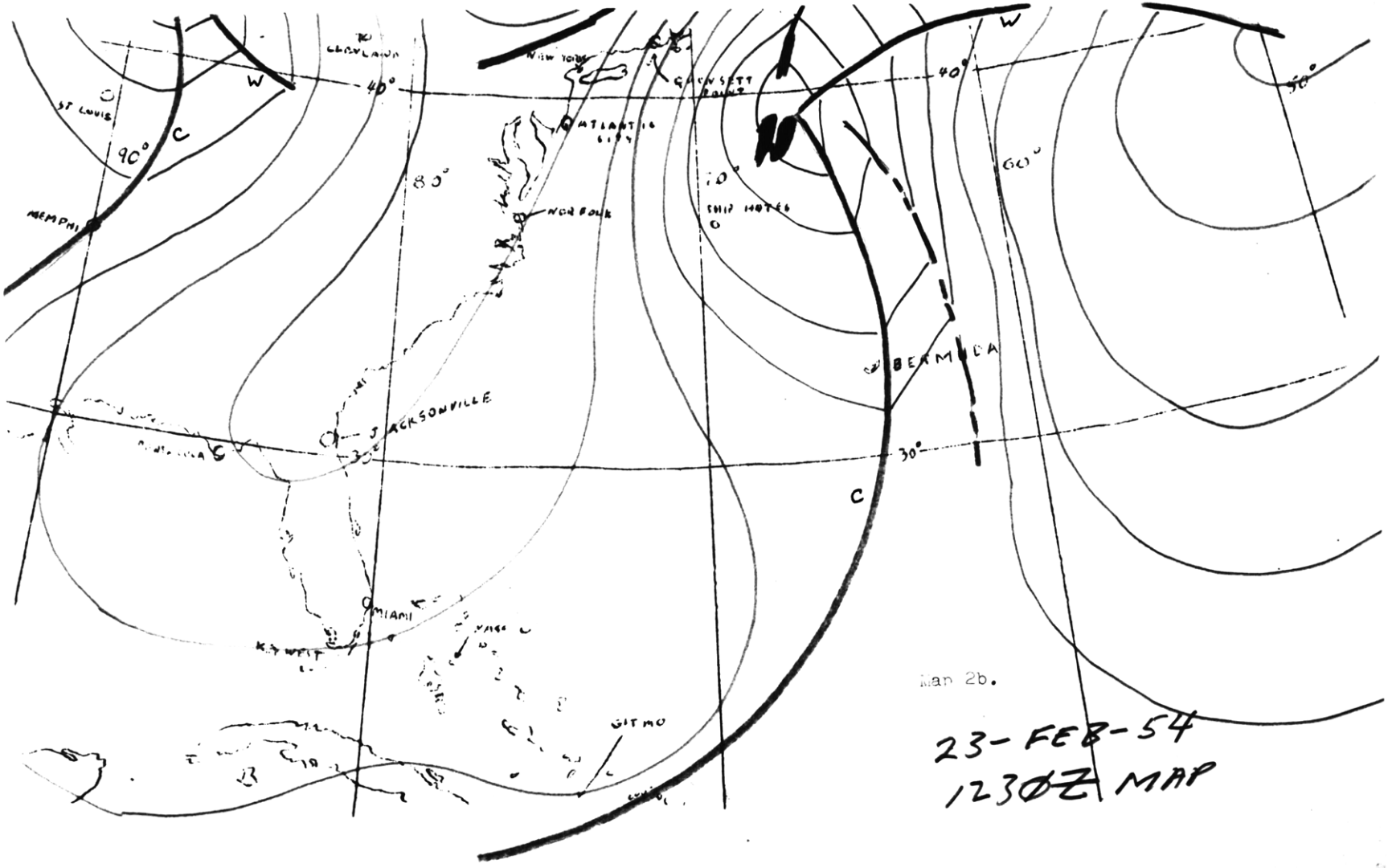
W
40°
90°
C
ST LOUIS
MEMPHIS
CLEVELAND
NEW YORK
ATLANTIC CITY
NORFOLK
80°
70°
60°
50°
W
CHIP HOTEL
BERMUDA
JACKSONVILLE
30°
C
MIAMI
KEY WEST
GITMO
Man 2b.
23-FEB-54
1230Z MAP

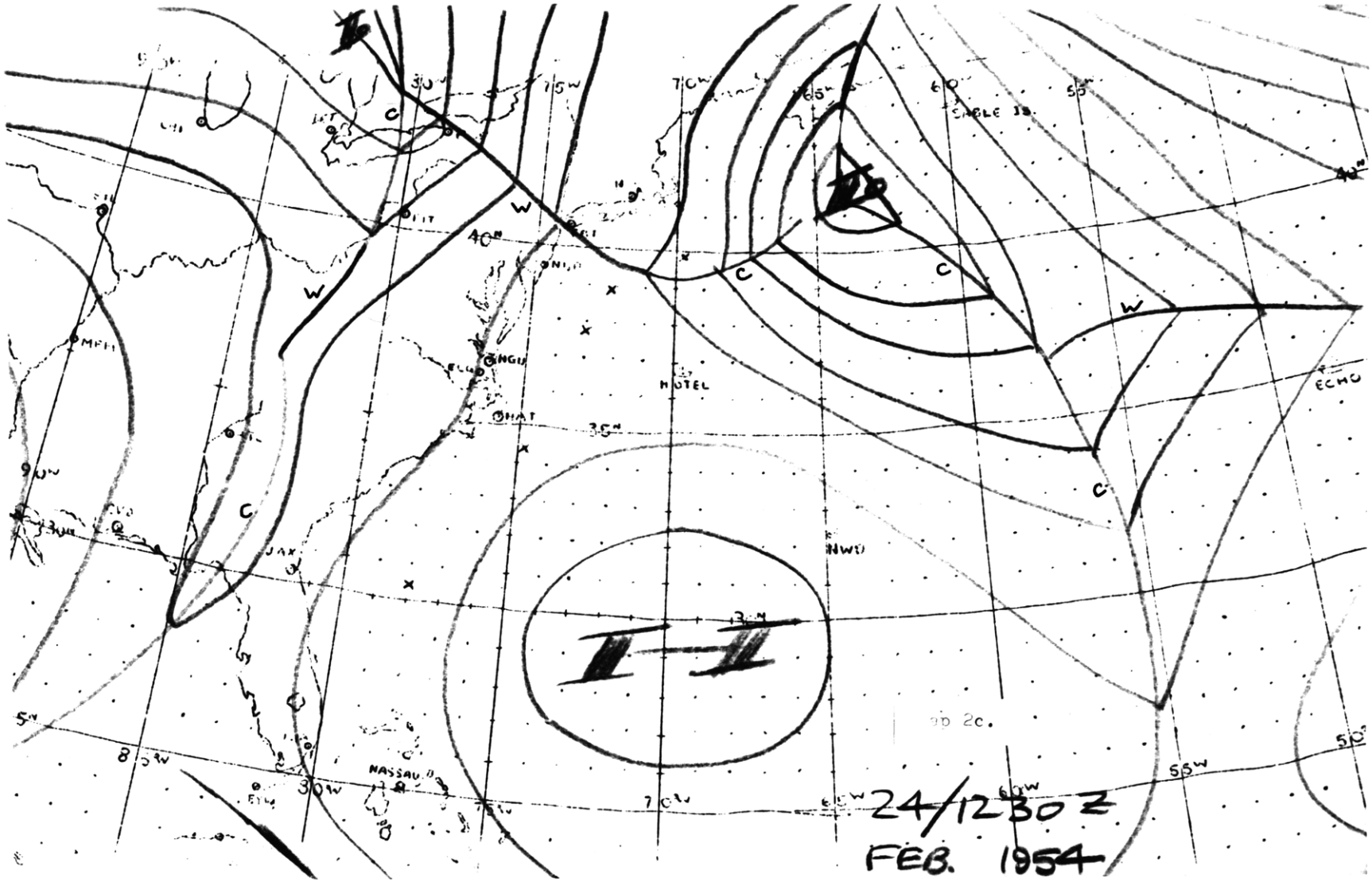
HOTEL
ECHO
NWS
JAX
MIA
NASSAU
24/1230Z
FEB. 1954

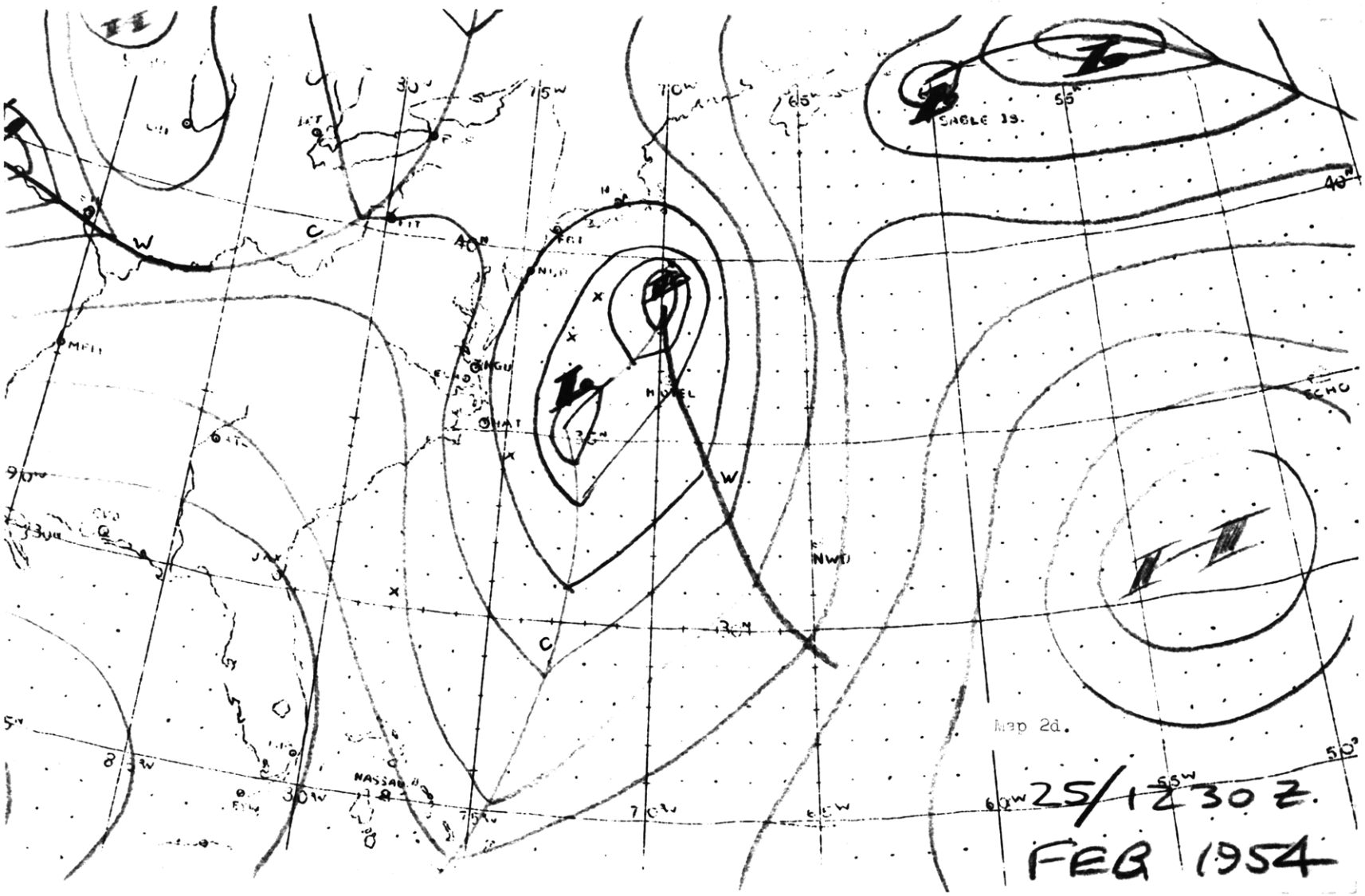
SABLE IS.
NWD
ECHO
Map 2d.
25/1230 Z.
FEB 1954

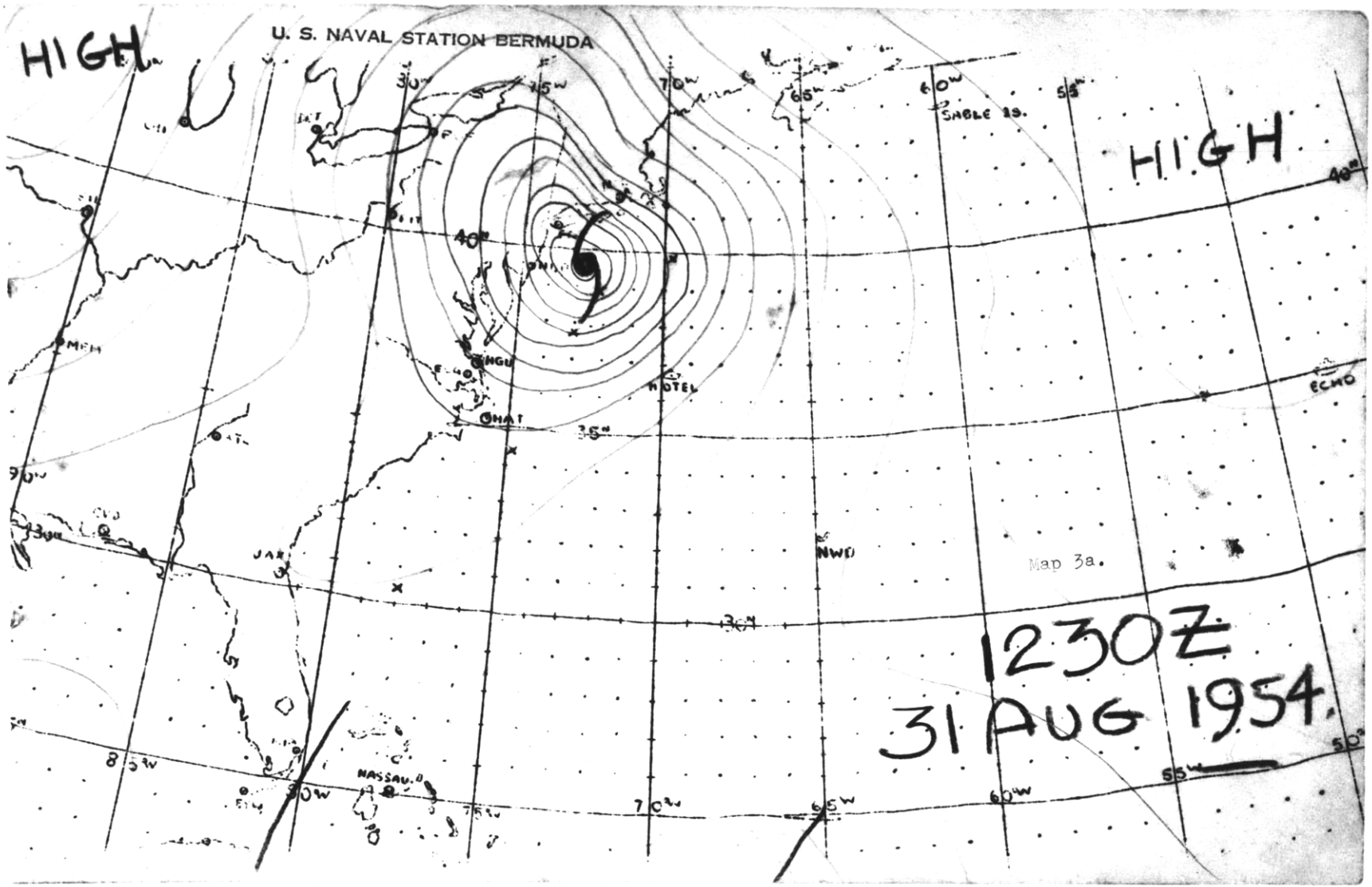
HIGH
U. S. NAVAL STATION BERMUDA
HIGH
SABLE I.
ECHO
HOTEL
INGU
CHAT
NWD
JAX
NASSAU
Map 3a.
1230Z
31 AUG 1954.

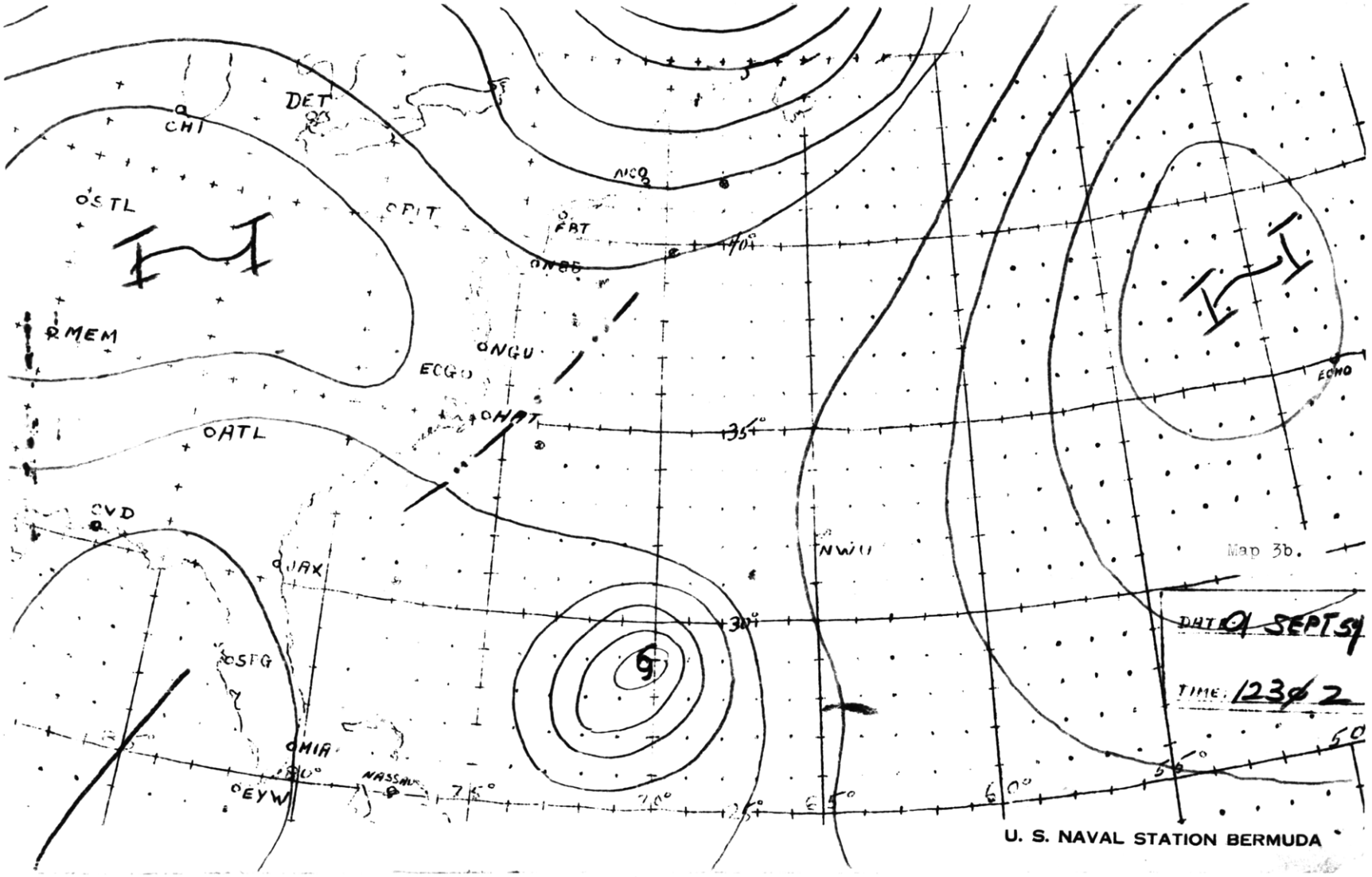
DET
CHI
OSTL
OPIT
NGO
FBT
RMEM
ONGU
ECGO
OHAT
OATL
CVD
OJAX
NWIL
Map 3b.
DATE 9 SEPT 54
TIME 1230Z
OSFG
OMIA
OEYW
NASSAU
ECHO
U. S. NAVAL STATION BERMUDA

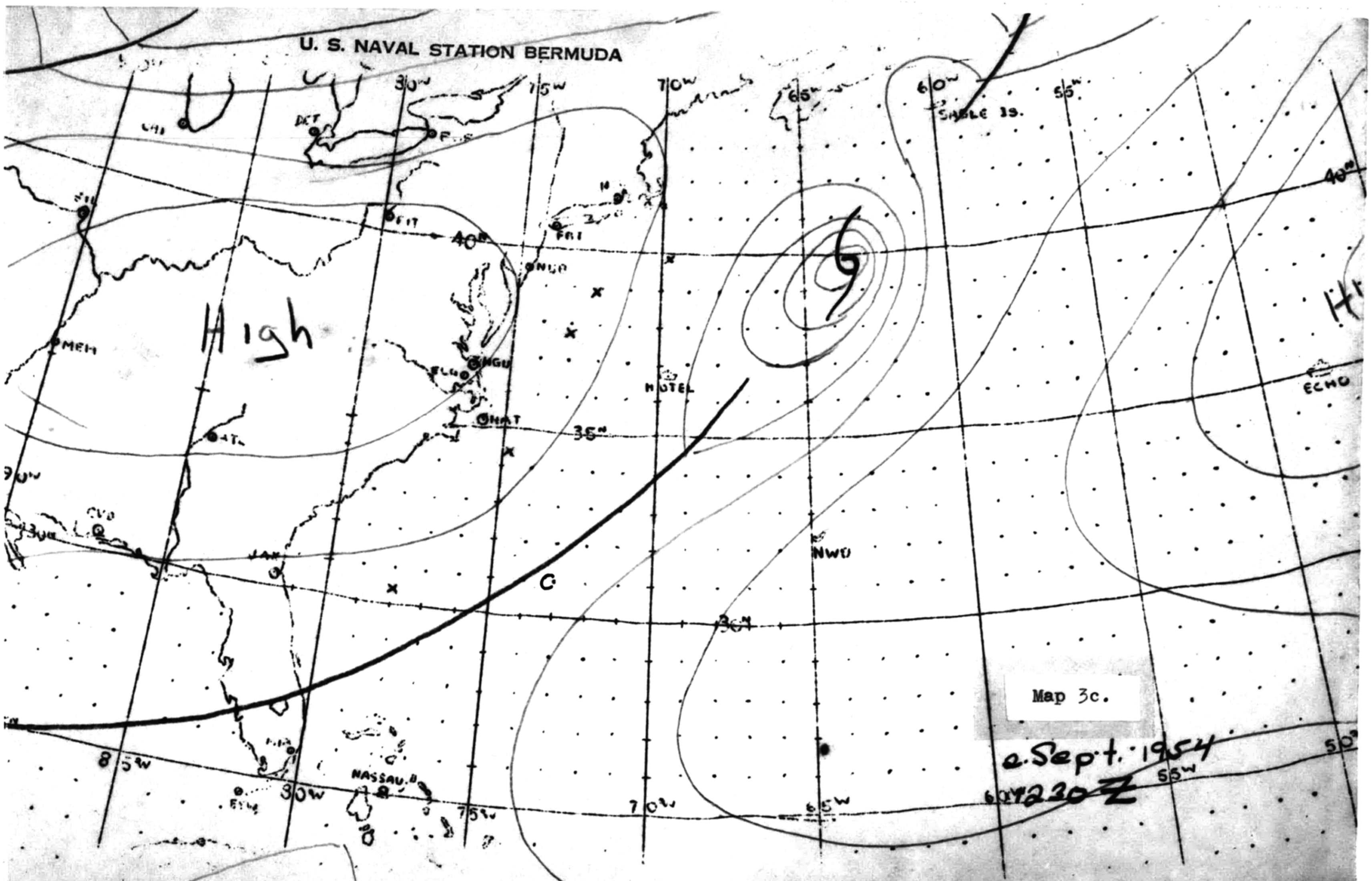
U. S. NAVAL STATION BERMUDA
Map 3c.
2 Sept. 1954
2230Z
High
C
HOTEL
ECHO
NWD
NASSAU
SABLE IS.
40N
35N
30N
85W
80W
75W
70W
65W
60W
55W
50W

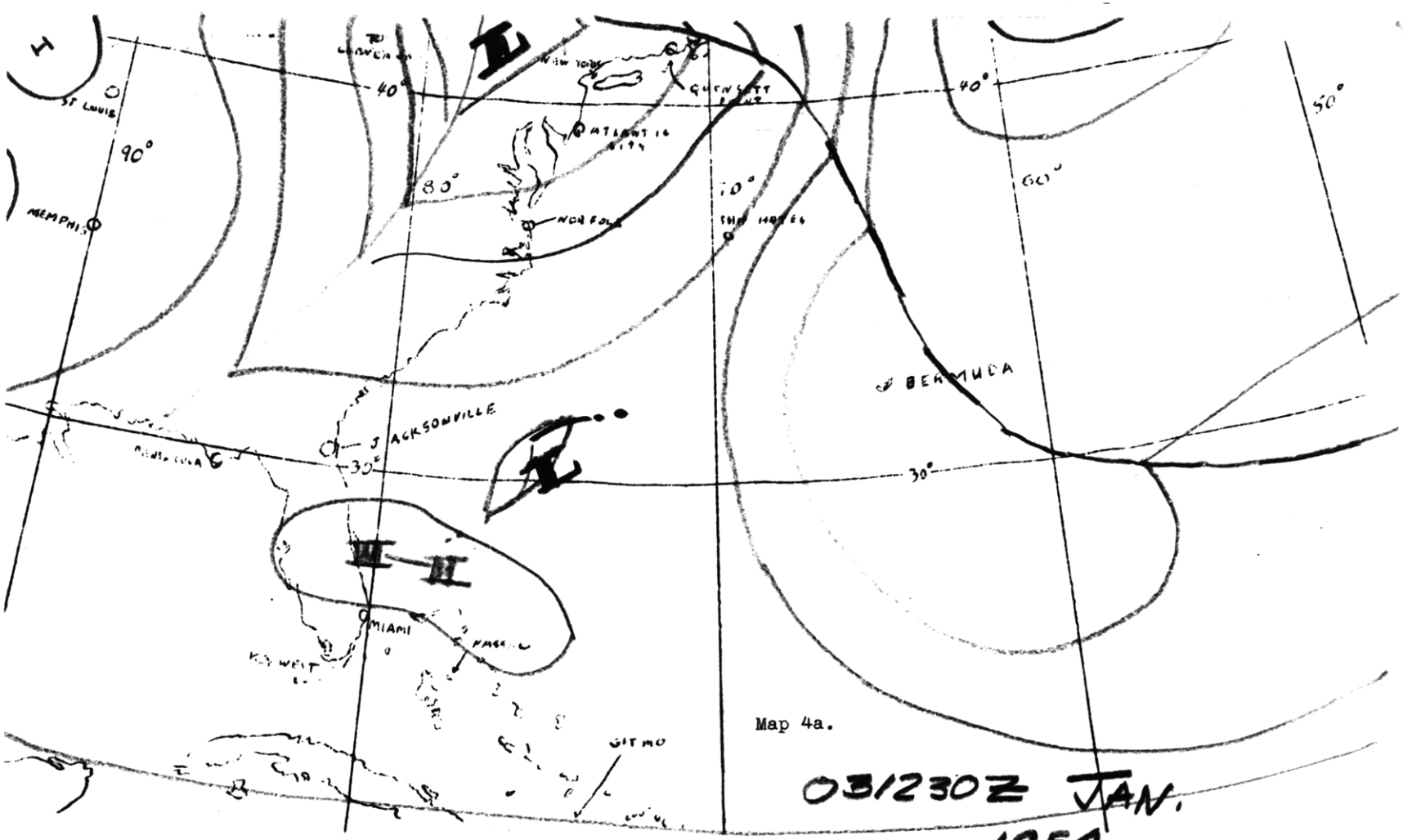

Map 4a.

031230Z JAN. 1954

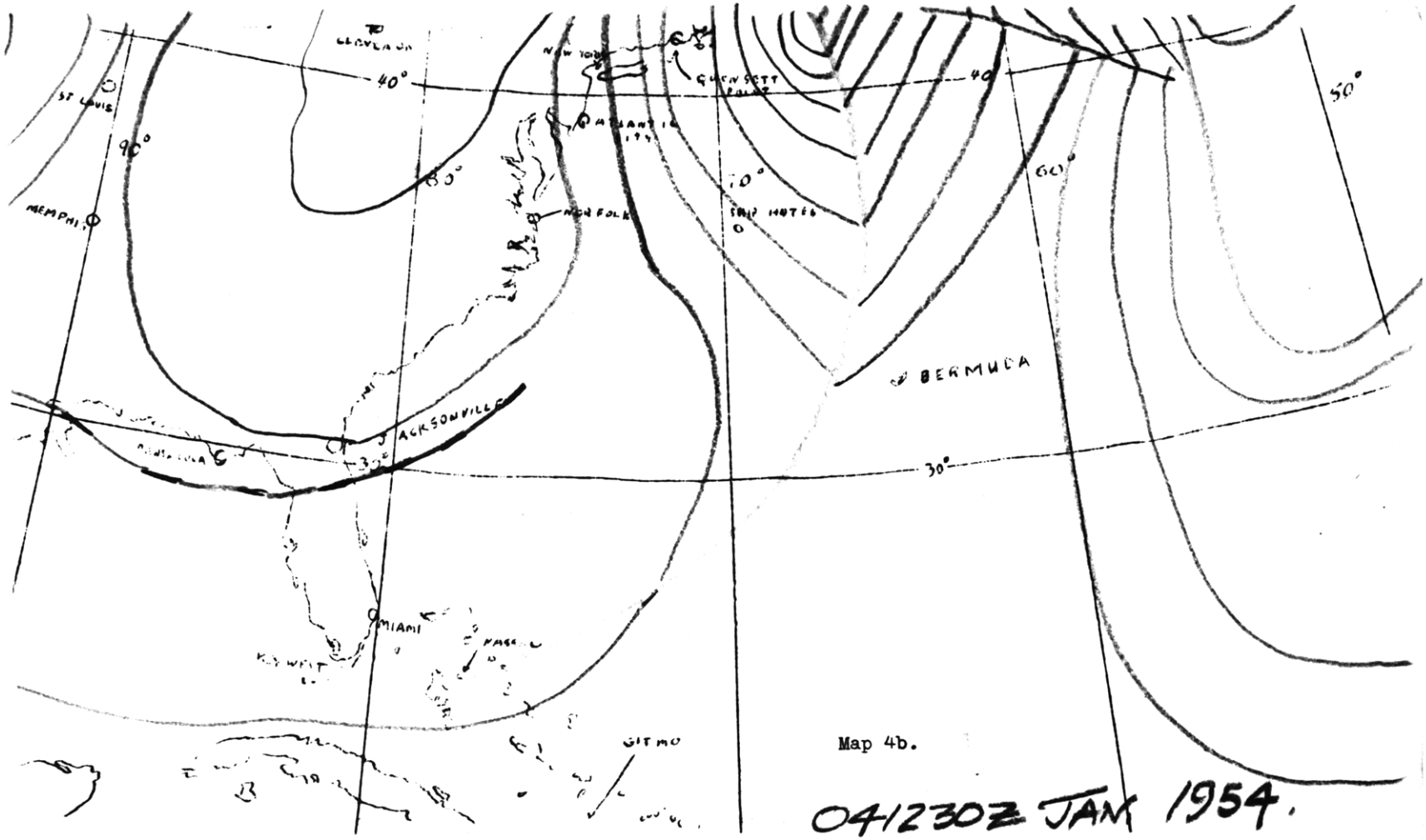

Map 4b.

041230Z JAN 1954.

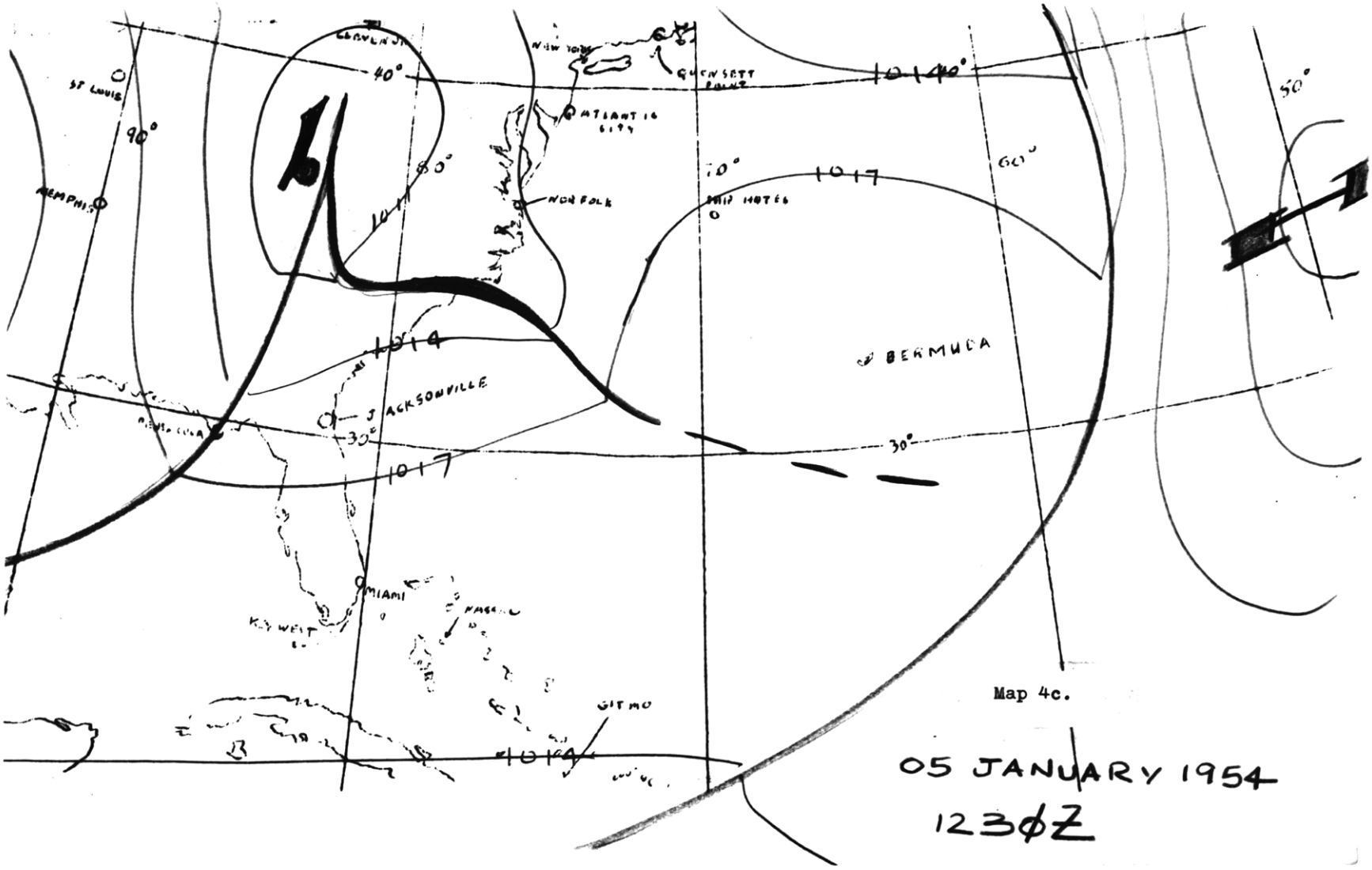

Map 4c.

05 JANUARY 1954

1230Z

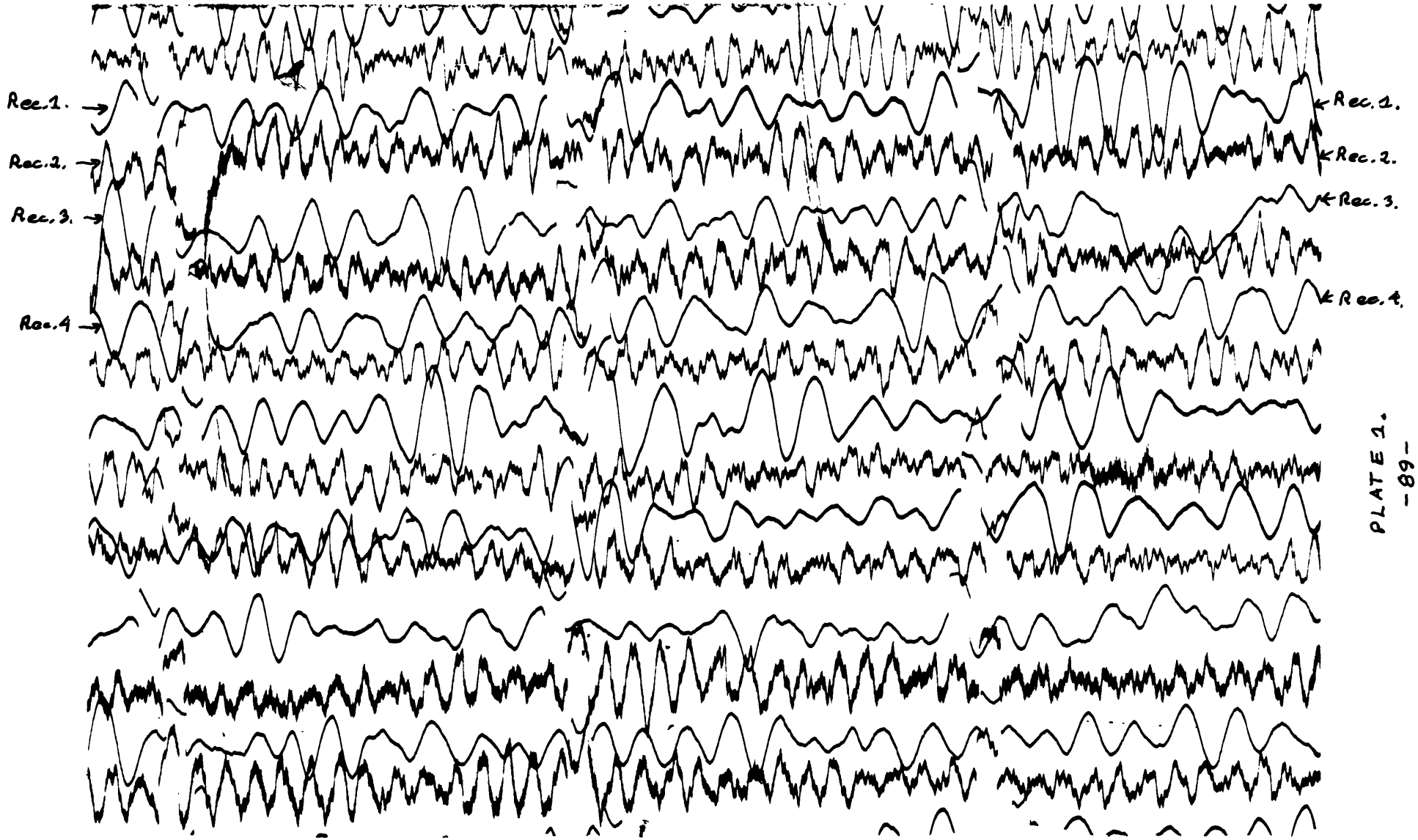

PLATE 1.

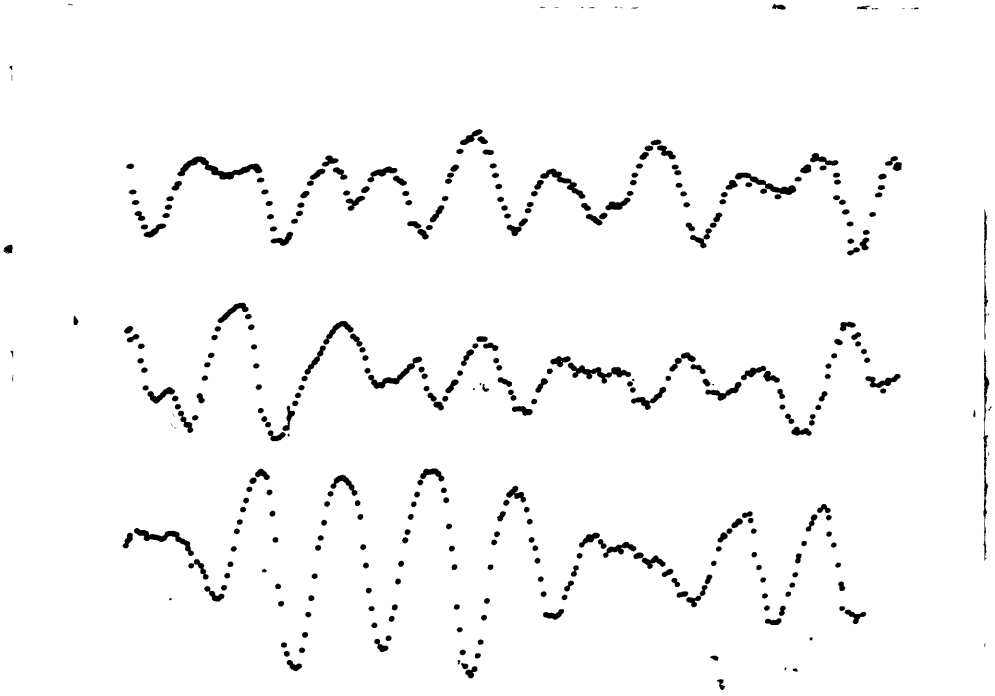

Record 1.

Record length - 3 minutes
Digitalization rate - 256 points per minute

There are points which seem misplaced here; this may be due to scope failure.

Plate 2.